RHEOLOGICAL STUDIES OF SILVER NANOPARTICLES BASED ISOTROPIC CONDUCTIVE ADHESIVE (Ag-ICAs) FOR MICROELECTRONIC PACKAGING APPLICATIONS

LIEW JIAN PING

MASTER OF ENGINEERING SCIENCE

LEE KONG CHIAN FACULTY OF
ENGINEERING SCIENCES
UNIVERSITI TUNKU ABDUL RAHMAN

AUGUST 2016

RHEOLOGICAL STUDIES OF SILVER NANOPARTICLES BASED ISOTROPIC CONDUCTIVE ADHESIVE (Ag-ICAs) FOR MICROELECTRONIC PACKAGING APPLICATIONS

By

Liew Jian Ping

A thesis submitted to the Department of Electrical and Electronic Engineering,

Lee Kong Chian Faculty of Engineering Science,

Universiti Tunku Abdul Rahman

in partial fulfillment of the requirements for the

Master of Engineering Science

AUGUST 2016

ABSTRACT

RHEOLOGICAL STUDIES OF SILVER NANOPARTICLES BASED ISOTROPIC CONDUCTIVE ADHESIVE (Ag-ICAs) FOR MICROELECTRONIC PACKAGING APPLICATIONS

Liew Jian Ping

Isotropic conductive adhesives (ICAs) have been widely studied by researchers in the electronics industry as an substitution to lead-based solders. ICAs have several advantages over commercial solder paste that includes environmental friendliness, lower curing temperature, finer pitch printing and easier processing. Nevertheless, it is still not possible to replace solder pastes completely with ICAs due to the limitations. The rheological behaviour of ICAs is one of the properties that have been studied most by researchers. There are many factors that influence the rheology of ICAs, including the filler size, weight fraction of filler, particle size distribution, shapes and surface roughness of filler. ICAs consist of polymeric material and filler particles/flakes such as silver.

All the finding reported on the rheological characterization of silver nanoparticles based isotropic conductive adhesives (Ag-ICAs) used in microelectronic packaging applications are separated into three major parts.

The first part of this study is to compare the fitting of viscosities for Ag-ICAs with empirical models namely; Power Law model and Cross model. The second part of this study, discuss the viscoelastic behaviour of Ag-ICAs samples by using oscillatory shear stress experiment. The last part of the work is focused on the study of the thixotropic behaviour of Ag-ICAs samples with both constant shear rate test and hysteresis loop test. In this study, the method of synthesizing silver nanoparticles in the lab was reported in order to obtain the targeted size range. The lab synthesize silver nanoparticles have a size range in between of 10 nm to 20 nm. The results shows that ICAs formulated with synthesize silver nanoparticles showed a high degree of thixotropic behaviour and highly elastic that leads to great recovery. ICAs with 0.8 weight fraction shows more solid-like behaviour and stable dispersion. In addition, Cross model fitted best with the experimental data with the highest correlation coefficients value, R^2.

ACKNOWLEDGEMENTS

First of all, I would like to express my appreciation to my supervisor, **Professor Dr. Rajkumar a/l Durairaj** for his guidance throughout this research. His valuable suggestions and knowledge was the main source which factoring the progress of my work as well as motivating me to put more efforts on this research. I would also like to express my appreciation to him for giving me freedom and positive attitude in completing this research. Throughout this research, my enthusiasm towards Material Science is increasing.

Secondly, I would like to acknowledge lecturer, Dr Liang Meng Suan for his valuable comments and advice on this research. Then, special thanks to my teammate and course mates for being so supportive and keep me motivated along the way.

I would like to thank my parents, Mr. Liew Hai Chew and Mdm. Ng Choon Lin for giving me financial support to complete my research program.

Finally, I would like to thank the staffs in Institute of Postgraduate Studies and Research (IPSR) and all the lecturers for their instrumental and education assistance.

FACULTY OF ENGINEERING AND SCIENCE

UNIVERSITI TUNKU ABDUL RAHMAN

Date:_____

SUBMISSION OF DISSERTATION

It is hereby certified that **LIEW JIAN PING** (ID No: **11UEM06774**) has completed this report entitled **"RHEOLOGICAL STUDIES OF SILVER NANOPARTICLES BASED ISOTROPIC CONDUCTIVE ADHESIVE (Ag-ICAs) FOR MICROELECTRONIC PACKAGING APPLICATIONS"** under the supervision of **PROF. DR. RAJKUMAR a/l DURAIRAJ** from the Department of Mechanical and Material Engineering, Lee Kong Chian Faculty of Engineering and Science, and **DR. LIANG MENG SUAN** from the Department of Mechanical and Material Engineering, Lee Kong Chian Faculty of Engineering and Science.

I understand that the University will upload softcopy of my thesis/dissertation* in pdf format into UTAR Institutional Repository, which may be made accessible to UTAR community and public.

Yours truly,

_____

(LIEW JIAN PING)

APPROVAL SHEET

I certify that, this project entitled **"RHEOLOGICAL STUDIES OF SILVER NANOPARTICLES BASED ISOTROPIC CONDUCTIVE ADHESIVE (Ag-ICAs) FOR MICROELECTRONIC PACKAGING APPLICATIONS"** was prepared by LIEW JIAN PING and submitted in partial fulfilment of the requirements for the degree of Master of Engineering Science at Universiti Tunku Abdul Rahman.

Approved by:

_____

(Prof. Dr Rajkumar a/l Durairaj) Date: _____

Supervisor

Department of Mechanical and Material Engineering

Lee Kong Chian Faculty of Engineering and Science

Universiti Tunku Abdul Rahman

_____

(Dr Liang Meng Suan) Date: _____

Co-Supervisor

Department of Mechanical and Material Engineering

Lee Kong Chian Faculty of Engineering and Science

Universiti Tunku Abdul Rahman

DECLARATION

I _____ hereby declare that the dissertation is based on my original work except for quotations and citations which have been duly acknowledged. I also declare that it has not been previously or concurrently submitted for any other degree at UTAR or other institutions.

_____

(LIEW JIAN PING)

Date _____

LIST OF PUBLICATION

1. Navindra, K., P., Nas, F., Athirah, N. A., Zaini, M. Z., Jamal, H., **Liew Jian Ping** and Durairaj, R., 2014. Antibiofilm properties of chemically synthesized silver nanoparticles found against Pseudomonas aeruginosa. *Journal of Nanobiotechnology*, 12 (2), pp. 1-7.

2. Durairaj, R., Chew, C.C., Tan, C.C. and **Liew Jian Ping**, 2013. Investigation of dynamic and mechanical thermal behavior of isotropic conductive adhesives. *Electronics Packaging Technology Conference***,** 11 – 13 December 2013, pp. 461-465

3. Durairaj, R., Lam, W.M., Kau, C.L., **Liew Jian Ping**, Ekere, N.N. and Lim, S.P., 2013. Rheological Characterisation of Diglycidylether of Bisphenol-A (DGEBA) and Polyurethane (PU) Based Isotropic Conductive Adhesives. *New Concepts, Applications and Methods*, pp. 23-38

4. Durairaj, R., Lam, W.M., **Liew Jian Ping**, Lim, S.P. and Ramesh T.S., 2013. Rheology and Processability of Diglycidylether of bisphenol-A (DGEBA) and Polyurethane (PU) based Isotropic Conductive Adhesives Filled with Different Size-distributed Silver Flakes and Silver Particles. *Engineering Letters*, 21 (3), pp. 143-148.

5. Durairaj, R., Lam, W.M., **Liew Jian Ping**, Lim, S.P. and Remesh T.S., 2013. Rheology and Processability of Diglycidylether of bisphenol-A (DGEBA) and Polyurethane (PU) based Isotropic Conductive Adhesives Filled with Different Size-distributed Silver Flakes and Silver Particles. *Proceeding of The 2013 International Conference of Mechanical Engineering, Imperial College London*, 3-5 July 2013.

6. Navindra, K.P., Ferina N., Athirah, N.A., Zaini, M.Z., **Liew Jian Ping**, Durairaj R., 2013. Inhibitory effect of silver nanoparticles on biofilm formation in pseudomonas aeruginosa. *International Conference on Nanoscience and Nanotechnology*, 1st -4th March 2013, Shah Alam, Malaysia.

LIST OF TABLES

LIST OF FIGURES

LIST OF ABBREVIATIONS

ACA	Anisotropic Conductive Adhesive
Ag	Silver
Au	Gold

CNT	Carbon Nanotubes
DGEBA	Diglycidyl Ether of Bisphenol-A
ECA	Electrical Conductive Adhesives
EDX	Energy-dispersive X-ray
FE-SEM	Field Emission Scanning Electron Microscopy
G’	Storage Modulus
G”	Loss Modulus
LMPA	Low-melting-point Alloy Fillers
LVER	Linear Viscoelastic Region
ICAs	Isotropic Conductive Adhesives
PCBs	Printed Circuit Boards
PD	Palladium
SMT	Surface Mount Technology
TMA	Thermo-mechanical Analysis
UV-Vis	Ultraviolet-visible

TABLE OF CONTENTS

CHAPTER 1

INTRODUCTION

1.1 Importance of isotropic conductive adhesives (ICAs)

Tin/lead based solders has been dominating the interconnect technology in electronics for decades. This industry pay a high attention on the toxicity of lead and its untoward effect on a human being health. Therefore, it is carefully being examined as the environmental awareness increased globally (Liu, 1999). Isotropic conductive adhesives (ICAs) are one of the favourable alternatives towards lead based solders as it has a relatively low curing temperature, a simpler processing procedure and the ease of forming bonds with different substance (Wong and Yi, 2006). There is a lot of different research going on all around the world for the past few years in order to produce an ICAs formulation with overall desired properties (Rusanen, 2000). Rheological properties of ICAs are one of the most important studies in the production of commercially used ICAs.

The deformation behaviour and viscosity of ICAs are rheological properties that have a significant influence on the microelectronic packaging printing process and the printing quality once printing is done. The printing of pastes will pass through a very fine apertures to print it on the printed circuit board (PCB) and might lead to unfinished transfer and clogging of ICAs to the PCB.

The consistency for the paste deposits from one board to another is not easy to maintain as the aperture size is very narrow and fine. In addition, the withdrawal of isotropic conductive adhesive is likely occur due to that as paste volumes reduce, the surface tension effects will be stronger than the over viscous flow. Thus, the rheological study of the isotropic conductive adhesive is a very essential parameter that will influence the printing process of the paste, the chances of paste withdrawal, and directly lead to the quality and durability of the solder joint (Bullard et al., 2009).

ICAs are a combination of conductive fillers which is the network for transportation of charge and polymeric binders that act as the mechanical strength. A polymeric matrix of an ICA formulation is usually epoxy resin. Epoxy based materials are broadly used as a major component in the engineering sector as they have excellent thermal and mechanical properties. The filler material for ICAs that is widely used is silver (Ag) that has high chemical stability and provides a better conductivity. The silver oxide also has a high conductivity. Moreover, it is convenient to formulate into a different range of measurable shapes and sizes. By applying the suitable selection of solvents, curing agent, plasticizers and accelerators will improve the desirable attributes of a ICAs.

1.2 Introduction to Electrical conductive adhesives (ECAs)

Electrical conductive adhesives (ECAs) are becoming more favourable in microelectronics packaging as it is more environmentally friendlier than solder paste. Electrical conductive adhesives in the market can be separated into two different types of conductive adhesives which includes anisotropic conductive adhesive (ACA) and isotropic conductive adhesive (ICA) (Gilleo, 1995).

Both types of ECAs consist of different materials, but both are a mixture of a polymer matrix and conductive fillers. For ACAs, the formation of electrical conduction usually occurs during the pressurization direction in the process of curing and the weight fractions of the conductive fillers in the formulation falls in between 5 and 10 weight percent. Thus, ACA is used for a finer pitch technology and is mainly used for fine pitch surface mount devices, flip chips and flat panel display applications (Wong and Lu, 2000). Usually, the ICAs contain conductive filler with a concentration between 60 and 80 weight percent and the adhesives formulated are able to conduct electricity in any directions (Perichaud et al., 2000). ICAs are widely used in surface mount technology and hybrid applications.

Conductive adhesives have the following advantages if compared with the conventional solder interconnection technology (Liu and Lai, 1998):

1) Finer pitch capability for ACAs;

2) Greater fatigue resistance and higher flexibility than conventional solder;

3) More environmental friendly than lead-based solder;

4) Lower curing temperature requirements;

5) Easier processing method as it does not require the use of flux;

6) The production cost may be lower by using cheaper substrates.

7) Non-solderable substrates such as glass can be used.

Even though there are many advantages by using ECA rather than conventional solder, the replacement of solder with this method is yet to be broadly used by the electronics engineering industry. It is due to that it has a poorer impact resistance, a lower electrical conductivity than solder paste and its long-term mechanical and electrical stability are weaker (Hvims, 1995; Liu et al., 1997). These are the few critical issues that have restricted a broader application of the electrically conductive adhesive technology. Researchers nowadays are currently conducting different studies to understand more about the mechanisms of these difficulties and finding ways to enhance the conductive adhesive performance for microelectronic applications in order to replace conventional solder (Rusanen, 2000).

1.3 Conduction Mechanisms in Isotropic Conductive Adhesives

In brief, there are two different ways to allow conductivity to conduct for ICAs as shown in Figure 1.1. First, the inter-particles contact within the polymer matrix itself is able to trigger the conductivity. The second path is by percolation. It associates the transportation of the electron within the matrix by quantum-mechanical electron tunneling between each individual particle that are closely packed together and allowing the breakdown of the dielectric in the matrix. The percolation is the principal of the conduction mechanisms in the early stages of conduction as suggested by researchers. When current is applied to polarize the conductive adhesive system, this will lead to the drop of electrical resistance by charge effects (Ritter, 1999). For instance, when currents continue to apply on it, the polarized particles will migrate and form more combination among each other. This will result the overwhelming percolation by the conduction of particle-to particle. Hence, turning it into a dominant conduction phenomenon.

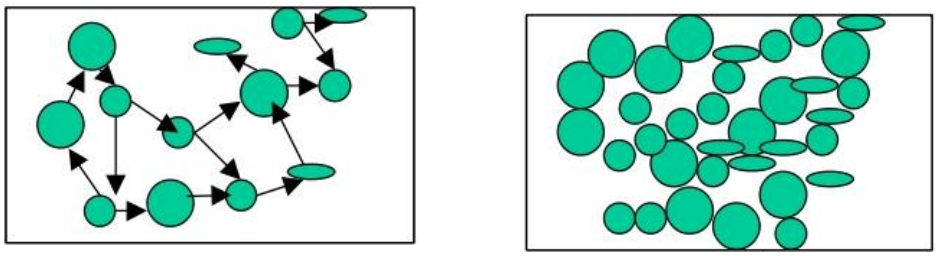

(a) (b)

(b)

Figure 1.1: Conduction Mechanisms in isotropic conductive adhesives; (a) Electron tunneling, (b) Particle-to-particle

1.4 Main issues of Isotropic Conductive Adhesives applications

Even though there are various possible usage and many advantages if compare with conventional solder for microelectronics applications and surface mount technology (SMT), problems and issues are yet to be clarified in order to fully replace solder by implementing ICAs in microelectronics packaging applications. Surface mount technology has high component availability, requires little process times, high yield, reliable joints for different components, and has the capability of repair and visual inspection of joints (Dahlback and Lundstrom, 1995). Electric conductive adhesives will not be an immediate replacement for solder at the moment for the use of current production lines. Primarily, it will not be cost effective in order to implement this is the market. To use ECAs in production, the lead plating and board conduction pas metallization must be improved. The material vendors, application companies and research organization need to work together in order to develop the standard components, materials and assembly equipment for a particular application. The development of new material must have a good mechanical bonding strength and electrical conductivity. The consistency of the stencil printing process and the accuracy of pick and placement machine need to be enhanced due to the finer pitch and thinner lead trends in the current market. Since the nature of ICAs is lack of self-alignment and non-selective wetting, they need to have additional rigid process requirement.

The limited accessibility of substrates and component that designed for adhesive is one of the major issues for using ICAs as a replacement for solder paste in the microelectronic packaging applications. Limited methods to ensure their relationship and the long term reliabilities to the speed up life time tests when solder joints is formulated with ICAs as a solder replacement. Multiples of mechanical electrical failure mechanisms involve each single property to monitor separately during a long lasting tests. The inspection of the adhesive joints by x-ray inspection methods or visually judging the quality of joints, which the work for each solder joints to produce perfectly are difficult to be done. The reworkability and reparability of adhesive joints must be studied and enhance to produce a better product.

1.5 Objectives

The aim of this study is to develop an isotropic conductive adhesive that has suitable rheological behaviour that can possibly act as a replacement for solder in the microelectronic packaging of electronic applications. The aims of this study include the subsequent measurable objectives:

1) To synthesize silver nanoparticles for ICA pastes.

2) To investigate the effect of filler size and weight fraction on viscosity and empirical modelling of silver nanoparticles based ICAs

3) To study the viscoelastic behaviour of silver nanoparticles based ICAs.

4) To investigate the thixotropic behaviour of silver nanoparticles based ICAs.

The subsequent research and development questions have been raised as specified below in order to accomplish the aims and objective of this study:

1) What are the effects of adding silver nanoparticles to the ICAs?

2) What are the effects of different particle sizes of silver nanoparticles added on the ICAs?

3) Comparing the ICAs formulated by commercials silver nanoparticles and lab synthesize silver nanoparticles, which is better?

1.6 Overview of the Thesis

Chapter 1 delivers the introduction of the study, the aim and objectives of the work, and shows an overview of the thesis. Chapter 2 presents the literature review on rheology of isotropic conductive adhesive pastes, linear viscoelasticity and thixotropic behaviour of the paste and the materials of ICAs. With regard to paste material, the weight fraction can also influence the viscosity of the paste. The viscosities of the ICAs can be quantified with the rheological model by some empirical models, namely Power Law model and Cross model to help us to understand how the ICAs perform in "Real World" (Agote et al., 2001). Consequently, the variation of the viscosity and weight fraction of ICAs with three types of fillers (silver flakes, synthesize silver nanoparticles and commercial silver nanoparticles) are investigated in this study. Lastly, the viscosities of the ICAs is compared and quantified by

empirical models mentioned above. The rheological measurements are necessary in the formulation of new pastes as the demand for lead-free pastes have increased significantly in the current market.

Chapter 3 introduces a description of the chemicals used, experimental equipment and parameters used for different parts of the study. In this study, the variation of rheology and weight fraction of ICAs with three types of fillers (silver flakes, synthesize silver nanoparticles and commercial silver nanoparticles) are investigated. The investigation is separated into three parts. Chapter 4 review the chemicals and method used use to synthesize silver nanoparticles as an ingredient for ICAs. In this study, concentrations of the chemical materials to synthesize silver nanoparticles are investigated.

Chapter 5 presents the relationship between viscosities and weight fractions of material paste which described by using empirical models, namely Power Law model and Cross model (Agote et al., 2001). Chapter 6 presents the second part is the study of linear viscoelasticity behaviour of the ICAs. This study is characterized by using oscillatory stress sweep test and the study of its phase angle.

Chapter 7 discussed the investigation of thixotropic behaviour of the ICAs which is the third part of the study. The final chapter, Chapter 8 presents the

summary of the study, the main conclusions from the study and the suggestions for the further work.

CHAPTER 2

LITERATURE REVIEW

2.1 Introduction

The related literature review on the rheological characterisation of ICAs used for microelectronic packaging application is presented in this chapter. The chapter includes three different parts. In the first part, it provides the reviews on the ICAs' rheological characterisation that is used for microelectronic packaging application. This part presents an overall literature that was done on the earlier work on the rheology of isotropic conductive adhesive. Three main sections were identified after reviewing these literatures: the viscoelastic behaviour of the adhesive, the thixotropic behaviour of the formulated paste and the correlation of viscosity with Power Law model and Cross model. The investigations in these areas are significant in order to understand paste behaviour throughout the microelectronic packaging process.

The second part reviewed the effect of weight fraction and filler size of filler on the rheology properties of the pastes. The investigation in this area will provide more understanding on the rheological test techniques in order to characterize the rheology properties of the paste. The final part provides a brief review on the thermoset epoxy resin that is used to formulate the ICAs.

2.2 Rheology

Rheology is used to describe the semi-solid and fluid properties of a material. It is defined as the science of the deformation and flow of matter. Initially the term “rheology” was created by Professor Bingham on 29 April 1929 at Columbus, Ohio for usage in chemistry and physics. The word itself originates from Greek, *rheos*, which means “flow”. Rheology can be used to describe the properties of a broad range of materials such as colloidal gases, oil, paints, concrete, foods, sludges and polymer. In brief, it is applicable to all types of materials from solids to gases (Gosta, 1995). All these materials are either exhibiting elastic behaviour (solid like behaviour) or viscous behaviour (liquid like behaviour) when external force is applied to them. The presence of both types of behaviour in a material indicates that this material is exhibiting a rheological behaviour, as it deform and flow at the same time. Commercial putty is one of the examples of viscoelastic material that exhibit both elastic and viscous properties simultaneously. At rest condition, putty exhibit elastic behaviour when it is at rest condition as it is motionless. However, when it is unloaded from the container, it exhibits viscous behaviour as putty able to flow out from the container.

The study of fluid movement and the stress placed on them is named as fluid mechanics. It is a branch of applied mechanics that concerned with the movement of dynamic and static of fluids. In another word, the movement of both liquid and gases (Andrew, 2001). A material can be categorized into three types of material, which are ideal solid, ideal liquid or viscoelastic material. An

ideal solid such as steel undergoes deformation when stress is applied. When the force is removed, the material then relaxes. The energy applied to it will be stored within the material and recovered during relaxation. On the other hand, an ideal liquid such as water will start to flow as stress is applied. However, it stops flowing right after the stress is removed from the material. The energy that's stored within the material will dissipate as heat. This is significantly different with an ideal solid. As mention earlier, a viscoelastic material will exhibit both solid behaviour and liquid behaviour when stress is applied to it (Andrew, 2001).

2.2.1 Basic terms associated with Rheology

2.2.1.1 Newtonian and non-Newtonian fluids

The Newton's law of viscosity describes the relationship between shear stress and shear rate as shown by the equation below.

$$\tau = \eta \dot{\gamma} \tag{1}$$

The symbol η, represents the Newtonian viscosity, $\dot{\gamma}$ represent the shear rate and τ represents shear stress. This simply means the viscosity of a Newtonian fluid remain constant regardless of the shear rate applied. In another word, the viscosity of the material is the direct proportionality against shear rate and shear stress. In brief, this indicates that even when the forces are applied on a

Newtonian fluid, it continues to flow continuously. Once the force applied is removed, the fluid will stop flowing. Figure 2.1 shows a plot of shear stress against shear rate for a flow curve of ideal liquid. Figure 2.2 presents a plot of viscosity against shear rate has where Newtonian fluid has a constant viscosity that is passing through the origin regardless the shear rate. Water and vegetable oils are examples of Newtonian fluids (Gosta, 1995).

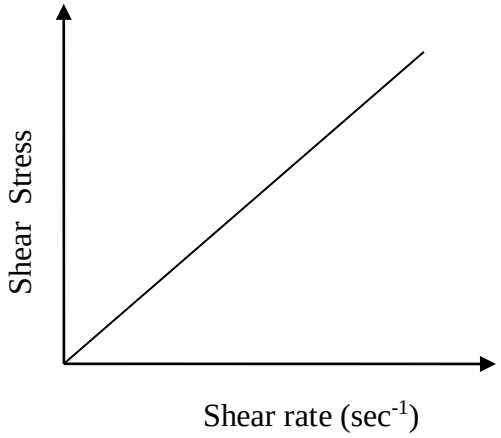

Figure 2.1: Flow curve of a Newtonian fluid

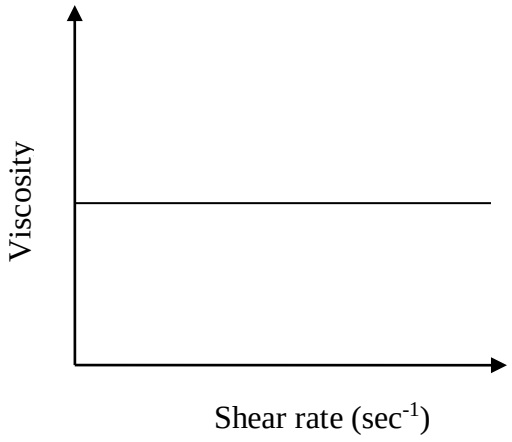

Figure 2.2: Viscosity curve of a Newtonian fluid

On the other hand, a non-Newtonian fluid has a viscosity that does not exhibit a linear relationship between shear rate and shear stress. Its viscosity changes as the shear rate change. Therefore, it is not possible to define a constant coefficient of viscosity for a non-Newtonian fluid (Mewis and Wagner, 2009). The ICAs material used in this study is a dense suspension. The ICAs materials are densely packed with particles that exhibiting continuous interactions between each particle. Hence, they will exhibit non-Newtonian flow behaviour as their viscosity will change as the shear rate varied.

2.2.1.2 Viscoelasticity

Material the exhibit both elastic and viscous characteristics when deformation starts as force is applied, this indicates that this material is viscoelastic in nature. Viscous materials such as water resist shearing deformation when stress is applied. For elastic materials, it starts to deform when stress is applied and return to original condition immediately once the stress is removed. In short, a viscoelastic material contains both of the properties and exhibiting time dependent strain. Linear viscoelastic region (LVER) of a sample must identified first before proceed with the in-depth dynamic measurements to probe its microstructure. LVER can be identified by performing the Amplitude Sweep Test, or also known as Oscillatory Stress Sweep Test. The length of LVER can determine the stability of a suspension. A sample that has a longer LVER indicates that it is well dispersed and a very stable system (Arild et al., 2012). A sample that is structurally stable required more shear in order for its elastic modulus to reduce or increase to a point that is lower or higher than is

viscous modulus. Furthermore, parameters such as Phase Angle (tan δ), Loss Modulus (G") and Storage Modulus (G') can be obtained by performing the oscillatory stress sweep test. Consequently, this allows us to characterize the viscoelastic properties of pastes, dispersions, slurries, emulsions, and gels (Mewis and Wagner, 2009).

ICAs that are formulated in this study are classified as a viscoelastic fluid. It exhibits the elastic behaviour (solid like) and viscous behaviour (liquid like) when shear is applied (Rusanen, 2000). The elastic property is described as the Storage Modulus (G'):

$$G' = \left(\frac{\tau_0}{\gamma_0}\right)\cos(\delta) = G''\sin(\delta) \tag{2}$$

and the viscous properties are describes as the Loss Modulus (G"):

$$G'' = \left(\frac{\tau_0}{\gamma_0}\right)\sin(\delta) = G'\cos(\delta) \tag{3}$$

The ratio between both properties is significantly essential. The phase angle (tan δ) is expressed by the quotient of G" and G':

$$\tan(\delta) = \frac{G''}{G'} \tag{4}$$

As mention earlier, as the force is applied on a structured viscoelastic system, the energy retained within the samples is elastic modulus and also known as storage modulus. The viscous behaviour (viscous modulus) will however loss up all the energy by dissipated as heat when force is applied. This is also known as loss modulus (Wilhelm, 2002).

The degree of viscoelasticity of the sample is correlated with Phase angle tan (δ). It is an indication of the strength of interaction within the material. Material that has a higher phase angle exhibits more viscous behaviour (Li, et al, 2014). Storage modulus of a paste that is in the process and after printing should be dominating. Hence, the tan (δ) value should be less than one (Lapasin et al., 1997). A material that has a high resistance from being separated and slumping has a high G' value as it is structurally more stable and has stronger interaction within the material. If the G' value is low, the paste most likely will lead to ski slopes or slow print speeds during production due to poor structural bonding. Therefore, it is very crucial to identify the storage modulus, loss modulus and phase angle of a ICAs before it went for mass production (Nachbaur et al., 2001; Arild et al., 2012).

2.2.2 Correlation of viscosity with Power Law Model and Cross Model

The definition of relative viscosity (η_r) is the quotient of the apparent viscosity of the suspension ($\eta_{\text{material paste}}$) and the pure binder ($\eta_{\text{resin}}$). Theoretical viscosity models such as Power Law or Ostwald de Waele Equation and Cross model

need to be fit with the experimental data so that the accuracy of the processing range for all the collected data can be determined.

2.2.2.1 Power Law Model

Power Law model:

$$\tau = K\dot{\gamma}^{n} \tag{5}$$

In Power Law, $\dot{\gamma}$ is the shear rate, τ is the shear stress, *K* is the consistency coefficient and *n* is the flow behaviour index that is dimensionless. The *n* value is known as the power law index. *K* describes the overall range of viscosities throughout the region of the flow curve that is being modelled. A fluid that is undergoing shear thinning will have a *n* value that is between zero and one. The closer the *n* value to zero shows that the sample undergoes more shear thinning. If a material has *n* value that equals to one, it exhibits Newtonian behaviour. Any *n* value that is bigger than one shows that the materials have shear thickening behaviour. The larger *n* value of a sample that is more than one shows that the sample undergoes more shear thickening. (Nguyen and Nguyen, 2012; Rao, 2014).

Thus, in terms of the viscosity, η as $\frac{\tau}{\dot{\gamma}}$,

$$\eta = K\dot{\gamma}^{n-1} \tag{6}$$

Most fluid that has a shear stress-shear rate plots are linear if plotted on a double logarithmic coordinates. By adding logarithms to both sides, the equation is now written as below:

$$\log(\eta) = (n-1)\log(\dot{\gamma}) + \log(K) \qquad (7)$$

It clearly shows that the plot of log η against log $\dot{\gamma}$ has a linear relationship. By comparing the experimental data and the predicted values of log η and log $\dot{\gamma}$ that derive from Power law helps to distinguish how closely the Power law model fit to the data obtain from the experiment. A study conducted by Evans and Beddow (1987) shows the experimental data that has a that has a shear rate range from 10^1 s^{-1} to 10^4 s^{-1} fits better into the Power Law model by using most of the viscometric or rheometry measuring devices in the market. Usually, the Power Law indexes and the magnitudes of the consistency of a formulated ICAs is dependent on the definite shear rate range that are selected in the test. Thus, more range of shear rate test needs to be done for different formulation of ICAs in order to identify the suitable range of shear rate to be used to fit in the Power Law plot. The main disadvantage of it is that it does not describe the high-shear and low-shear rate constant-viscosity data of a suspension that undergoes shear-thinning (Rao, 2007).

2.2.2.2 Cross Model

Cross model:

$$\eta = \eta_{\infty} + \frac{\eta_{0} - \eta_{\infty}}{1+\left(\frac{b}{a}\dot{\gamma}\right)^{m}} \tag{8}$$

In Cross model, the zero shear viscosity, η_0 is an important property that able to evaluate the making of an assessment for the suspension's stability. The *m* is the parameter or the rate constant in Cross model. Same as Power Law, it is dimensionless and also provides the measurement for the degree of dependence of viscosity on shear rate for a material that undergoes shear-thinning region just like Power Law index. If the *m* value is more than zero, this indicates that the increase of shear rate lead to a decrease in viscosity. Hence, material that has *m* value higher than zero is exhibiting a shear thinning behaviour. The value of $\frac{b}{a}$ is the consistency coefficient in Cross model. Cross model is useful to describe the shear dependence of materials over a broad range of shear rates (Koskul and Nabialek, 2004).

2.2.3 Introduction to Thixotropy

Every viscous fluids are exhibiting thixotropic behaviour. When shear is applied on viscous fluid, the structure will start to break down and resulting a decrease in viscosity. However, once the shear is removed, immediately it will

recover back to the original state. Hence, thixotropic refers to the finite time needed for the material recover back to original state after shear is removed as per process above. There are some materials that stay as solids when the stress applied is very small but turns into liquid state when stress applied is big. The material will then settle back to original state once the applied stress is removed. (Barnes, 1997; Ineke, 2003).

Thixotropy is commonly evaluated by quantifying the enclosed region between the up-and-down curves that collected in an increasing and decreasing of shear rate over time. Figure 2.3 shows an example of the enclosed region obtained from a hysteresis loop test (Barnes, 1997). The area between the loops is a measurement of the 'amount' of thixotropic behaviour in the fluid. In addition, it is also an indication of energy has loss during the test cycle that has been used to break down the material's structure. Nevertheless, the hysteresis area is a relative measure of thixotropic as it depends on the nature of the material and parameters that express the hysteresis loop test. The parameter includes the maximum shear rate and the total duration of the linear increasing and decreasing of shear rate (Elaine et al., 2006).

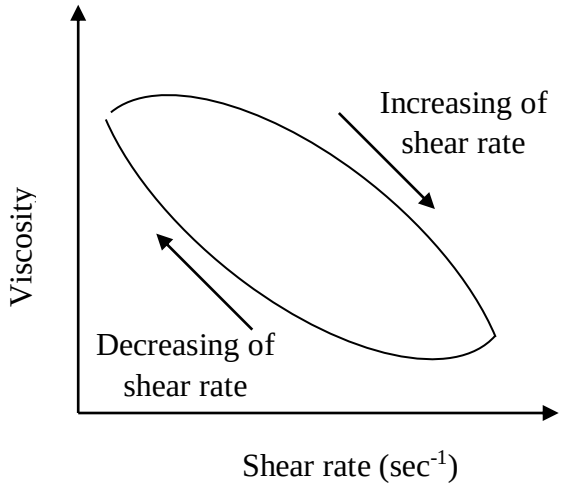

Figure 2.3: Hysteresis loop obtained by increasing of shear rate and decreasing of shear rate

A material that has a large hysteresis loop indicates that it has a high degree of thixotropy. In brief, this material has a large structural change when shear is applied and the structure rebuilt after shear is removed. Usually, this is due to the weak attractive forces between the particles within the material. The weak bonding between particles can be broken down easily when the mechanical stresses are applied during flow. Hence, as shear applied is increasing, the viscosity of the material drops at the same time. Once the shear is slowly removed, the weak bonding between the particles will rebuild at the simultaneously. Therefore, the viscosity of the material increase as the shear starts to decrease. In this scenario, the kinetic coagulation is the driving mechanisms. However, this mechanism requires a restricted amount of time and shear for us to observe the hysteresis loop (Mewis and Wagner, 2009). The poor recovery of the formulated ICAs may result poor stencil printing during

the production microelectronic packaging. This may lead to the paste will easily squeeze out and slump might occurs. However, if the minimum of time or the minimum amount of shear for the material to break down has not reach, the hysteresis loop will not present. Therefore, it is significantly important to study the thixotropic behaviour of the formulated ICAs with the respect to in printability in industrial usage.

2.3 Previous studies on rheology of pastes (solder paste and ICAs)

The rheology of solder pastes and ICAs are mainly affected by the rheology of flux system and the conductive fillers particles characteristics that include particles size, particles size distribution and weight fraction or concentration of the filler. Many studies have been conducted by researchers in order to have a better understanding of their rheological properties as it will directly affect the printing performance during manufacturing (Lu and Wong, 2008).

In McGrath et al. (2008) study, he combines a few different methods to review the properties of an epoxy composite. He includes dynamic shear rheology, thermo-mechanical analysis (TMA), scanning electron microscopy (SEM), and fracture toughness testing to have a full understanding of the epoxy composites. This allows him to identify the chemical, mechanical, thermal, and fracture properties of the epoxy composites. In his study, the epoxy fracture properties such the average filler size, particle shape, loading, size distribution and paste

crosslink density are the variables before proceeding to the test. His results indicated that even a slight change in particle size, size distribution and shape will also affect the final properties of the epoxy composites. The broadening of the shear storage modulus-temperature profile was more noticeable in the lower crosslink density. McGrath et al. (2008) mentioned that this is due to increasing of filler concentration; it increases the connections among the particle-particle within the system. This study discusses the importance of the shape of the particle, loading, filler size, paste crosslink density and their influences on the rheology of paste.

A study conducted by Zhang et al. (2010) reviewed one of the more important parameters, which is the influence of particle size distribution on rheological properties of solder pastes. The printing performance will be significantly affected by the solder paste particle size distribution. He suggested that parameters such as size ratio and concentration of fillers must be tested to identify the respective relationship between them with the rheological properties of the paste. This study found out that as the size ratio increase and the particle concentration remains constant, the viscosity of the paste will decrease only at low shear rates. However, when the size ratio is constant, the increasing of particle concentration will increase the viscosity. His result clearly shows that the concentration or weight fraction for the fillers and the particle size will significantly affect the viscosity of the solder paste. Zhang et al. (2010) mentioned that a better understanding of solder paste rheological properties will improve the printing process and it will also change the after print behaviour of the paste that include the slump resistance and tack value.

The viscosity of the paste must be low enough to squeeze out from the squeezee but at the same time high enough for it to reshape itself after it removed from the squeezee.

Kim et al. (2003) also conducted a study on rheological properties of solder pastes. As mention earlier, the rheological properties of a paste can directly affect the printing performance. In this study, he highlighted the solder paste rheology is one of the most important parameters that will affect the printing process and the reflow soldering performance. This statement is clearly in the same agreement state by Zhang et al. (2009). In Kim et al. (2003) research, they found out that the viscosity of a disperse suspension increase as the weight fraction of the suspended solder particles increases. The viscosity increases immediately by increasing the solder particle concentration. This shows that the interaction between the flux system and particles exhibit a significant influence on the viscosity of the solder pastes. Therefore, an oscillatory test is needed to study the liquid and solid (G' and G") characteristics of solder paste that is beyond the linear viscoelastic region.

Jon (2009) conducted a study on the thixotropic behaviour of paste. He mentioned that as shear is applied to a thixotropic system, the viscosity will reduce. If the shear applied is higher, the more noticeable drop in the viscosity of the paste. This is the result of a structural breakdown within the systems occurs when the shear is applied. It is attributed to the process of breaking down the linkages between the fillers in the suspension. The bonded particles

have relatively weak attractive forces among each other. This leads to a space filling particulate network. Hence, these weak inter-particle bonds can be broken down by mechanical stresses applied during flow, which is the shear applied. In addition Mewis et al. (2009) reviewed the thixotropic behaviour for particulate suspensions. His result shows that the particle network breaks down into separate flocs when stress applied. He also found out that the further increase of stress applied will lead to a further size reduction on the flocs. This is in the same agreement with Jon (2009). However, as the shear rate is reduced, the bonding between the particles in the network will rebuild and hence its structure will reconstruct. As a result, viscosity of the paste increases with the decrease of shear rate. Yet, it requires a certain amount of time for the network to reconstruct after they were broken down. Is it therefore, the study on thixotropic behaviour for a paste is significantly important as it allow us to understand the recovery of the paste after shear is applied. A paste that has poor recovery may result in slump during the printing process.

The creep-recovery test is the time-dependent deformation of a material that is loading constantly. In brief, a constant stress is applied to the sample in the shear direction to observe the stain in a period of time. Once the strain of the material becomes constant, the stress is removed immediately. This time dependent behaviour, which is the thixotropic behaviour will show by the sample (Goertzen and Kessler, 2006). As mention above, this behaviour is crucially important for us to understand before further proceed the formulated ICAs for industrial usage. With the help of this test, the tendency for the paste to slump can be correlated with the relaxation in strain immediately right after

the stress is removed. Bao et al. (1998), Nguty et al. (2000) and Goertzen and Kessler, (2006) used the creep-recovery test to study the slump tendency for different pastes. Their studies on the viscoelastic behaviour of pastes discuss that more research regarding the solid and liquid characteristics of the pastes especially on a linear viscoelastic region of pastes needs to be identified to have a better understanding of the materials thixotropic behaviour.

ICAs are a viscoelastic material that contains both viscous and elastic behaviour. In Arash (2012) study, he clearly indicates that the loss modulus, G'' and storage modulus, G' rise when the weight fraction of the additives of the epoxy matrix was increased. As he increases the shear rate is increased, the matrix viscosity decreases intensely too. This is due to that the structures of the matrix are build up by weak bonding among particles that can be broken down easily by shear. He mentioned that if the shear rate is too high, this will totally break down the contacts of the particles in the system. Hence, the viscosity of the matrix will reduce significantly. In addition, there is no thixotropic behaviour at this moment because the three-dimensional network structure gets completely ruptured completely. These findings were well aligned with the study by Malucelli et al. (2007). By understanding the behaviour of the ICAs at higher stress allow us to improve the formulation to be used in the printing process.

2.4 Materials of ICAs

The environmental awareness has increased nowadays and the manufacturer needs alternatives for solder paste in electronic packaging. ICAs are one of the most promising alternatives for solder paste. By using ICAs, the disposal problems produce by solder paste can be reduced significantly as ICAs are lead free material (Ifran and Kumar, 2007). Moreover, ICAs only required a low temperature processing if compare to solder paste. Hence, with a lowered curing temperature than solder paste, this will reduce the manufacturing cost effectiveness (Cheng et al., 2007). Yet, more research need to be done in order to have a better understanding of the reliability, design, material, and manufacturing characteristics of all kinds of conductive adhesive technologies before a valuation of their leverages as a component attachment permanent replacement can be made. It is because the current ICA materials in the market have low electric conductivity and has weak mechanical properties (Omar, 1991). However, ICAs are conducted in all directions by increasing the filler concentration (Lu and Wong, 2008). Consequently, for this time being, ICAs implementations are restricted to low cost applications and applications where solder paste is not an option to use. Thus, researches have been focusing on evaluating both the mechanical and electrical of ICAs for microelectronic packaging processes (Liu, 1999).

2.4.1 Conductive Filler

In current research, ICAs are incorporated with different types of metal fillers to be used in manufacturing. There are few factors that affect the choice of metal fillers in the ICAs formulation. Commonly, silver flakes are used in formulating ICAs. First, it has high resistivity towards corrosion and more durability. Even though gold is also a metal that has high resistivity towards corrosion, but it is very expensive. Silver is highly conductive and has high chemical stability that will provide a better functionality for the formulated ICAs (Liu, 1999). Liu (1999) also mentions that even the silver content in ICAs oxidized after the expose to heat and humidity, the silver oxides still remain highly conductive. However, this is not the case for others metal, for example copper. Therefore, silver is widely used as conductive filler in the formulation of isotropic conductive adhesive. Nickel is another material that has high resistivity towards oxidation, but the experimental data shown that nickel is not able to fabricate into optimized geometries during ICAs production (Shimada et al., 2000). As mentioned earlier, most ICAs in current industry have poor mechanical properties. Thus, some researchers tend to incorporate carbon nanotubes (CNTs) in the formulation of ICAs as CNTs is able to enhance the mechanical properties of the ICA (Yim and Kim, 2010).

A research conducted by Kusy (1977) mentioned that silver coated plastics or glass particles is able to use as a metal filler, but the method use for mixing processes is to fragment the fragile silver coating. The interaction between the

metal particles will be weakened and lead to a poor performance in conductivity. Nevertheless, formulated ICAs must have great performance in conductivity and as a result, silver that is coated in layers are not suitable to be used in ICAs formulations.

Shimada et al. (2000) mentioned that another important element to use silver as a conductive filler is that silver can be easily obtain or synthesize into an extensive range of controllable shapes and sizes. The extensive range of silver that may be present as flakes or particles can effectively increase conductivity over a narrow size distribution. As the voids within the formulated ICAs can reduce or filled by the overlapping flakes and different sizes of silver particles. This eventually allows all the flakes and particles that are different in sizes to overlap within each other so that electric can conduct effectively in microelectronic packaging.

Another study conducted by Rebeca et al. (2010) has reviewed that influence of silver nanoparticles size in electric conductivity. The filler particle, silver nanoparticles in the isotropic conductive adhesive (ICAs) will uniformly distribute and then built a network within the polymer structure after it is cured. This will allow the current to pass through these network and hence, allowing the mixture to electrical conductive. In addition, the current is able to flow in any direction due to its nature. His study concludes that as the sizes of silver nanoparticles increase, the electric conductivity increases too.

A research conducted by Kottaus et al. (1997) found out that the thermo-mechanical properties of the adhesives by using the porous silver power were improved since the infiltration of the resin into the pores occurs. The electric conductivity of these porous silver powder systems is not sufficient enough to be used in microelectronic packaging. ICAs formulated with porous silver power must improve its electrical performance before it does for manufacturing.

Kim et al. (2009) mentioned that the volume ratio of conductive filler, silver flakes, will significantly affect the electrical conductivity of a ICAs. It is due to that the volume ratio will directly determine the reaction rate for the conductive fillers to react with the insulating surrounding, the epoxy of the formulation. As the volume ratio of conductive filler increase, the thermal conductivity of the ICAs increases too.

The study by Lu and Wong (2000) show by mixing silver flakes with a low-melting-point alloy fillers (LMPA) to formulate the ICAs will lead to a good metallurgical connection between all the conductive fillers within the formulated ICAs. When the ICAs is undergoing curing, the alloy fillers melt and connected all the silver flakes and hence, metallize the entire substrates. This eventually resulting a high conductivity property for the formulated adhesives.

In Shimada et al. (2000) findings, it is easier to control the sizes for silver condutive filler by synthesize them with stock materials. Thus, the synthesis of silver nanoparticles is important as we able to control the sizes by changing the parameters during the silver reduction process. It is crucial to study how different sizes of silver nanoparticles as they may form different bonding strength with epoxy and significantly affect the printing performance of the paste and its electrical properties. The weight fraction is another important factor that will affect the conductivity (Kim et al., 2009) of the paste and its printing ability too. Thus, the paste need to prepare in different weight fraction to identify which formulation exhibit a better rheology properties that may improve the performance during mass production in the industry.

2.4.2 Thermoset Epoxy Resin - DGEBA

Epoxy thermoset are one of the best materials that is widely used for microelectronic packaging due to its good thermomechanical properties and simple processing method (Zheng et al., 2010). A study conducted by Lyons (1991) reviewed that due to the interlocked cross-linked structure after cure, thermoset materials do not flow at high temperatures. Thermoset polymers are monomers but will start polymerize during the curing process. After curing, it will form a dimensional cross-linked molecular structures, as the branch points will restructure form bonding with the polymer chains. The various numbers of branch points are named as the cross-link density.

The epoxy resin used in this study is synthesized by reacting bisphenol A and epichlorohydrin, which are the common ingredients for liquid adhesives. It is 2,2-bis[4-(2'3' epoxy propoxy) phenyl] propane or also known as diglycidyl ether of bisphenol-A (DGEBA) and its molecular structure is shown in Figure 2.5.

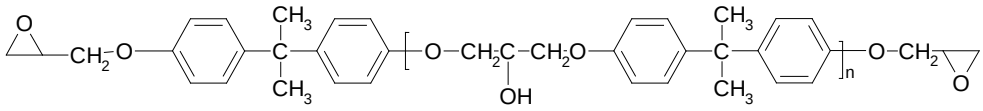

Figure 2.4 Molecular Structure for Diglycidyl Ether of Bisphenol-A (DGEBA) (Bryan et al, 1999)

One of the main characteristic of epoxy resin is that modification to the base resin can be done by changing its epoxy equivalent weight of the base resin. For DGEBA, it has an epoxide functionality of 2 for its average molecular weight of 380. DGEBA resin has low viscosity and has a high crosslink density and reactivity. In an epoxy system, it must contain a curing agent and the resin itself. Figure 2.5 shows that the diglycidyl ether of bisphenol-A resin contains active member rings and it can be opened to form high cross-linked structures when it is undergoing a curing process **(**Bryan et al., 1999). DGEBA epoxy resins can be cured by a mainly three types of curing agent that includes catalytic that is Lewis acids and bases, anhydrides, and amines such as aliphatic and aromatic. These different types of curing agent will lead to different product properties, various rates of curing and several curing mechanisms. Therefore, in order to obtain the desired product that undergoes

certain reaction in a specific temperature, the curing agent play act as an accelerator (Bearbeitet, 2010).

CHAPTER 3

MATERIALS AND METHODS

3.1 Introduction

This chapter describes the chemical materials used, experimental equipment, and parameters used for several parts of the study. In this study, the rheology and weight fraction of ICAs formulated with three types of fillers (silver flakes, synthesize silver nanoparticles and commercial silver nanoparticles) were investigated. The investigation was divided into four parts. Chapter 4 will present the results and discussion for lab synthesis silver nanoparticles that was used in the formulation of ICAs. This enables us to identify the differences between commercial silver nanoparticles and lab synthesis silver nanoparticles. Two empirical models, namely Cross model and Power Law model were utilized to describe the relationship between viscosities and weight fractions of formulated ICAs. The results and discussion of this study will be presented in Chapter 5. The study of linear-viscoelasticity established on oscillatory stress experiments is presented in Chapter 6. Lastly, Chapter 7 shows the investigation of thixoptropic behaviour of the formulated ICAs.

3.2 Methodology

Approximately 0.2 by the weight fraction of epoxy resins and 0.8 by the weight fraction of fillers were weighed and mixed. Then, the mixture was mixed well for 20 minutes in a beaker. Later, proceed with rheological properties characterizations that include Oscillatory Stress Sweep Test, Hysteresis Loop Test, Thixotropy Recovery test or also known as Steady Shear Rate Test and Empirical Modelling Test. The earlier steps are repeated with all other samples with 0.4 by the weight fraction of epoxy resins and 0.6 by the weight fraction of fillers. Figure 3.1 shows the flow chart for the methodology for the sample testing in this study.

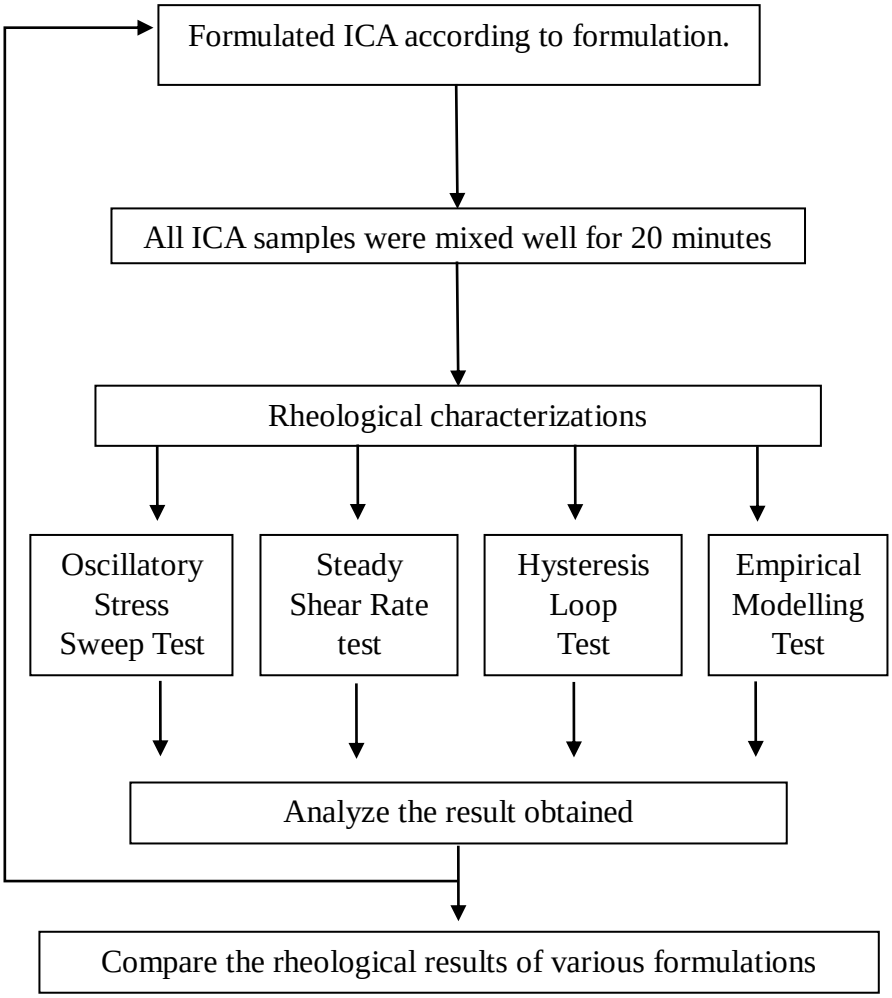

Figure 3.1: Flow Chart for Methodology

3.3 Sample preparation

In this study, the viscosities of formulated silver nanoparticles based isotropic conductive adhesives (ICAs) at a different weight fraction of filler were investigated. It is significantly important to perform the experiments on the silver nanoparticles based ICAs at room temperature. Thus, the silver nanoparticles based ICA samples were rest at for 20 minutes before performing any of the rheological tests.

Table 3.1 shows the chemicals used in the formulation of ICAs. As for Table 3.2, it shows the parameters being investigated in these studies were the size of filler and weight fraction of filler. Composition of silver nanoparticles based ICA's samples investigated is shown in Table 3.3.

Table 3.1: Chemicals used in the preparation of ICAs

Chemical Functions	**Chemicals**	**Manufacturer**
Resin	Diglycidylether of bisphenol-A (DGEBA)	Sigma Aldrich
Fillers	Silver flakes	Sigma Aldrich
	Commercial silver nanoparticles	Sigma Aldrich
	Synthesis silver nanoparticles	-

Table 3.2: Size and weight fraction of filler investigated

Filler size				**weight fraction of filler**
Silver flakes	**Commercial silver nanoparticles**		**Synthesize silver nanoparticles**	
10 µm	10nm	20nm	10 to 20nm	0.6
				0.8

Table 3.3: Samples investigated

Samples	Formulation					
	Epoxy		Filler 1		Filler 2	
S1	DGEBA	40%	Silver Flakes	60%	-	
S2	DGEBA	40%	Silver Flakes	50%	Commercial Silver Nanoparticles (10nm)	10%
S3	DGEBA	40%	Silver Flakes	50%	Commercial Silver Nanoparticles (20nm)	10%
S4	DGEBA	40%	Silver Flakes	50%	Synthesized Silver Nanoparticles	10%
S5	DGEBA	20%	Silver Flakes	80%	-	
S6	DGEBA	20%	Silver Flakes	70%	Commercial Silver Nanoparticles (10nm)	10%
S7	DGEBA	20%	Silver Flakes	70%	Commercial Silver Nanoparticles (20nm)	10%
S8	DGEBA	20%	Silver Flakes	70%	Synthesized Silver Nanoparticles	10%

3.4 Rheometry

All of the flow curve test measurements were performed with the Physica MCR 301 controlled stress rheometer (Anton Paar). The rheometer setup was shown in Figure 3.2. The formation of wall slip at the interface between the plate and isotropic conductive paste will affect the precision of the result. Thus, parallel plate geometry with a diameter of 25mm was chosen in this study. The gap height of 0.5 mm was used between the upper and lower plate, as shown in

Figure 3.3. Before placing the sample onto the rheometer, the ICA was stirred for 5 min to ensure that the material structure is consistent with the particles being well distributed into the adhesive. Then, the formulated isotropic conductive paste samples were rested at about 20 minutes before proceed to the rheological tests. The sample was loaded on the rheometer's peltier plate and the geometry plate was lowered to the gap of 0.5mm after that. The excess pastes surrounding the plate edges pastes that squeezed out by the geometry plate were carefully trimmed using a micro spoon. Later, the sample was allowed to rest for approximate 1 minute to ensure to reach the equilibrium state before the testing start. All tests were performed at 25˚C where the temperature is controlled by the Peltier-Plate system. Every test was repeated for three times for stabilization with fresh samples for every repeated test. Table 3.4 shows the experimental parameters set for the flow curve test. Flow curves are basic rheology characteristics that representing the static properties of a flowing material. It expresses a relation between shear rate and shear stress that was applied to the viscosity of a material, which flows. Table 3.5 shows the experimental parameters set for the oscillatory that enable us to study the viscoelastic properties of the pastes. Table 3.6 and 3.7 shows the experimental parameters set for steady shear rate thixotropic and hysteresis loop tests.

Table 3.4: Experimental parameters for flow curve test

Experimental values				
Initial shear rate (s^{-1})	**Final shear rate (s^{-1})**	**Number of measuring point**	**Interval between measuring point (s)**	**Overall Duration (s)**
0.001	100	31	3	100

Table 3.5: Experimental parameters for the oscillatory stress sweep test

Experimental values				
Strain (%)	**Angular frequency (s^{-1})**	**Number of measuring point**	**Interval between measuring point (s)**	**Overall Duration (s)**
0.001-100	10	25	5	125

Table 3.6: Experimental parameters for the steady shear rate test

Experimental values					
Initial shear rate (s^{-1})	**High shear rate (s^{-1})**	**Number of measuring point**			**Overall duration (s)**
		Interval 1	**Interval 2**	**Interval 3**	
0.01	10	20	10	20	210

Table 3.7: Experimental parameters for the hysteresis loop test

Experimental values				
Initial shear rate (s^{-1})	**High shear rate (s^{-1})**	**Number of measuring point**		**Overall duration (s)**
		Up curve	**Down curve**	
0.01	10	20	20	200

3.5 Field Emission Scanning Electron Microscopy

The investigation of the micrograph of the silver nanoparticles is done by using the Field Emission Scanning Electron Microscopy (FE-SEM). The model of the FE-SEM used in this project is JEOL JSM-6701F FE-SEM. FE-SEM is a powerful tool for the study of morphology and topography, chemistry or in-situ experiments of a material. In brief, FE-SEM works by having a field-emission cathode in the electron gun of a scanning electron microscope that delivers the narrower probing beams at low and high electron energy. The emitted electron energy is then collected by the detector and compared with the primary beam's intensity to produce an image. As a result, it will not only improve the spatial resolution, but also minimized the sample charging and damage towards the sample.

A drop of the colloidal silver nanoparticles is placed on carbon coated adhesive tape and dried in a few minutes. The sample is then placed in the sputter coater to be coated with gold plasma. This is to minimize the charging effect of metallic samples.

CHAPTER 4

SYNTHESIS OF SILVER NANOPARTICLES

4.1 Introduction

The focus of this study is the chemical synthesis of silver nanoparticles and study the influence of silver nanoparticle's size on the rheological properties for the formulated ICAs. As in every aspect of the production of silver nanoparticles based ICAs for microelectronic packaging, cost is always the most important consideration. The purpose to synthesize silver nanoparticles in the lab is not only to reduce the production cost of silver nanoparticles based ICAs but also to produce a colloidal silver nanoparticle solution with a range of different sizes. The cost of commercial colloidal silver nanoparticles solution from the manufacturer is significantly higher if compare to stock material for the synthesis silver nanoparticles. With this, it will highly reduce the production cost for such silver nanoparticles based ICAs. Moreover, the performance of ICAs that are formulated with synthesized silver nanoparticles that has a range of different sizes can be compared with ICAs that contain only commercial silver nanoparticles. Therefore, the chemical synthesis of silver nanoparticles and energy dispersive X-ray analysis was conducted in this study.

4.2 Results and Discussion

The synthesis of silver nanoparticles from silver salts have been done by varieties of chemical reduction methods (Arnim and Michael, 1999; Andreescu et al., 2007; Solomon et al., 2007). The silver salt described in this study is silver nitrate as the initial stock material. Since borohydride is highly reactive, its handiness if compared with gaseous hydrogen and it is also nontoxic, which makes the borohydride reduction the most broadly used methods to prepare silver nanoparticles (Krutyakov et al., 2008). In addition, using cold sodium borohydride to reduce silver nitrate is one of the famous methods to synthesize silver nanoparticles (Fang, 1998). Therefore, this method is used in this study to synthesize silver nanoparticles. It requires a large excess amount of sodium borohydride to reduce the ionic silver and also to stabilize the formed silver nanoparticles. This reduction formula of silver nitrate by sodium borohydride can be written as (Solomon et al., 2007):

$$AgNO^3 + NaBH^4 \rightarrow Ag + \frac{1}{2}H^2 + \frac{1}{2}B^2H^6 + NaNO^3 \qquad (9)$$

In most of the studies that are using sodium borohydride to reduce silver nitrate, the colloidal silver nanoparticles is prepared as bright yellows. Clear yellow colloidal silver nanoparticles can be obtained subjected upon the duration of the reaction with ice cold sodium borohydride (Holter et al., 1998). With the references to literature, the expected particles sizes fall in the region of 7-20 nm

in diameter (Bönnemann and Ryan, 2001; Solomon et al., 2007; Krutyakov et al., 2008). Moreover, the absorbance lies approximate close to 420 nm with a peak width at half maximum (PWHM) of 50-70 nm (Solomon et al., 2007). The entire synthesis process to obtain colloidal silver was handled carefully, especially handling the strong reductant, sodium borohydride. Appropriate cleaning of laboratory equipment is important and it is crucial to make sure the silver nitrate solution did not expose to the aqueous sodium borohydride before the mixing start.

All equipment was cleaned thoroughly by soaking in ethanol and rinsed with distilled water. A stock solution of silver nitrate ($AgNO_3$) and sodium borohydride ($NaBH_4$) were prepared before mixing process. 679mg of $AgNO_3$ (molar weight = 169081 g/mol) was dissolved in 400ml distilled water to prepare 10mM aqueous silver nitrate solution. Furthermore, 20mM of aqueous sodium borohydride solution ware prepared by adding 302mg of $NaBH_4$ (molar weight = 37.83 g/mol) to 400ml distilled water. Both compounds dissolved easily within a few minutes. The concentration of the sodium borohydride solution was twice of the silver nitrate solution is to ensure the stability of the colloid solution as suggested by Solomon et.al. (2007).

The mixing was done in a 50ml beaker. 3ml of aqueous silver nitrate contained in a 10ml beaker was added drop by drop into 9ml of aqueous solution sodium borohydride, using a dropper. Before mixing, both solutions were cooled down

to 4 degree Celsius in an ice bath. A magnetic stirrer was used to ensure the solution stirred vigorously throughout the whole reaction.

Throughout the addition of the silver nitrate to the aqueous sodium borohydride solution, a light yellow colour gradually appeared in the mixture. This indicates the formation of silver nanoparticles. Figure 4.1, shows the colloidal silver that synthesized in this experiment. Later, 1M of aqueous silver nitrate solution and 2M of aqueous sodium borohydride solutions were prepared to compare the formed silver nanoparticles solutions with result from the low concentration of both stock solutions. The mixing procedures were repeated as per mention earlier. Throughout the addition of the silver nitrate to the aqueous sodium borohydride solution, the entire reduction is very aggressive. The equilibrium of the reduction reaction shifts to the right and cause the formed silver nanoparticles agglomerate together into a solid state particle. Figure 4.2 shows the agglomerated silver nanoparticles formed with high concentration silver nitrate solutions and sodium borohydride solution. Therefore, in order to produce colloidal silver nanoparticles, it has to be prepared with low concentration of aqueous silver nitrate and aqueous sodium borohydride as high concentration reagents will lead to agglomeration of silver nanoparticles immediately.

Figure 4.1: Synthesized silver nanoparticles in colloidal solution formulated with low concentration of stock material

Figure 4.2: Agglomerated synthesized silver nanoparticles formulated with high concentration of stock material

4.3 Characterization of Silver Nanoparticles

4.3.1 Particle Size Measurement Using FE-SEM

The Field Emission Scanning Electron Microscopy (FE-SEM) (JSM-6710F) is used to investigate the colloidal silver solution. Figure 4.4 show that the sizes of the synthesized silver nanoparticles. After comparing all the images captured, the synthesized silver nanoparticles sizes falls in a range of 10-20 nm. The synthesis of silver nanoparticles from the reduction of sodium borohydride with silver nitrate has produced silver nanoparticles that are in the same size range as described in literature (Solomon et al., 2007; Krutyakov et al., 2008).

The increasing of the silver nitrate precursor volume will eventually reduce the relative volume of the reductant which is the sodium borohdyride in this colloidal system. In brief, the borohydride acts as a surfactant to stabilize the silver nanoparticles that is produced in this reaction. The entire repulsion mechanism is illustrated in Figure 4.3. The amount of sodium borohydride presents in the solution during the reaction is very significant. The present of low amount of sodium borohydride in the solution will allow the formation of larger silver nanoparticles before the borohydride adsorption on the silver nanoparticles starts. Thus, the amount of borohydride must be adequate enough to stabilize the silver nanoparticles. However, too much of sodium borohydride in the system will increase the ionic strength of the solution that leads to stimulating aggregation of the particles. This will lead to the borohydride

shields the charges, then letting the particles to clump together. As a result, the formation of aggregated particles occurs. Hence, the molar ratio of 1:2 between silver nitrate and sodium borohydride is set for this reduction (Bahadory, 2008).

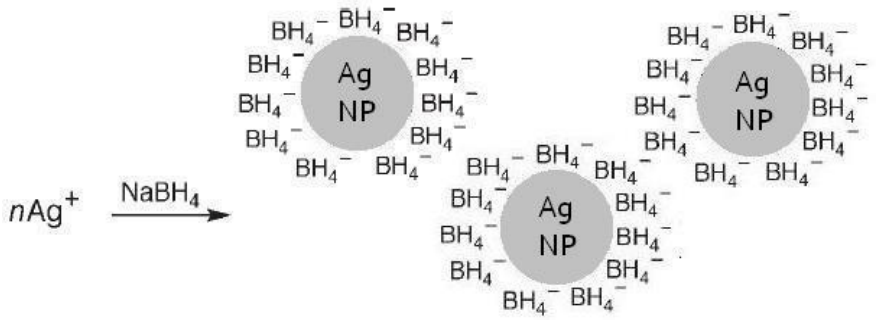

Figure 4.3: Repulsive forces between the adsorbed borohydride ensures separation of the silver naoparticles

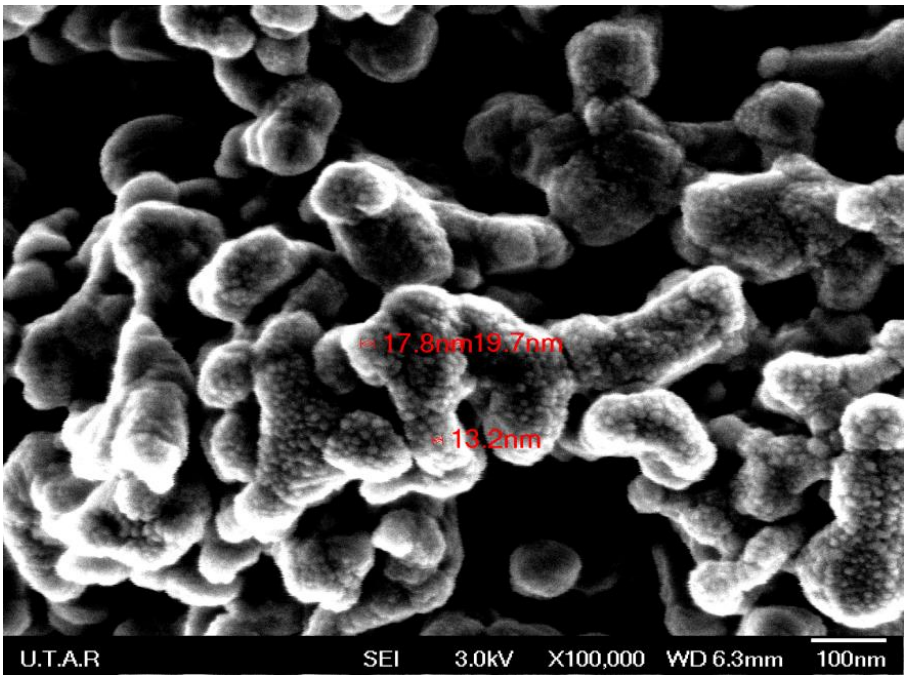

(a)

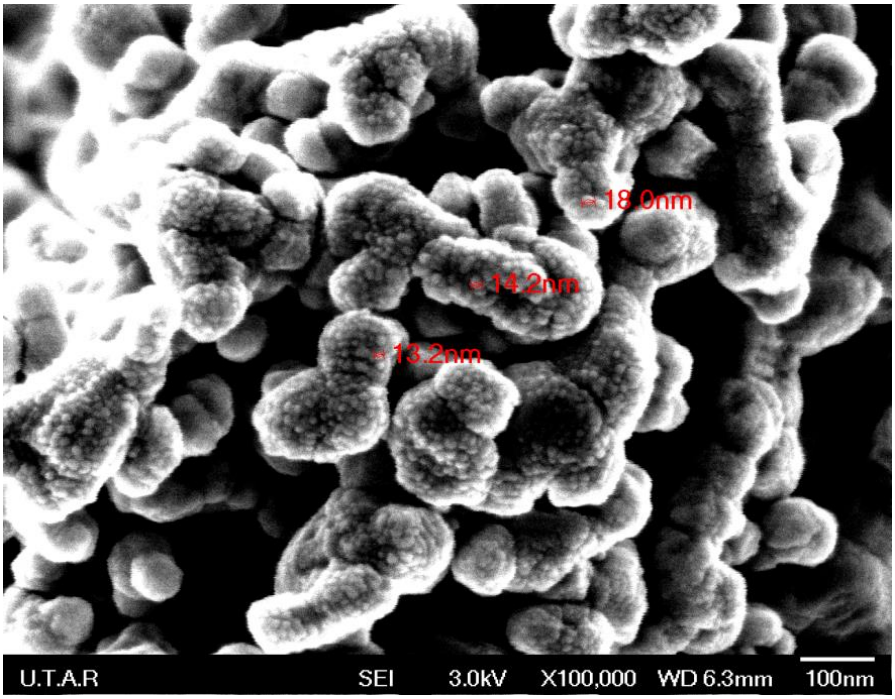

(b)

Figure 4.4: Silver nanoparticles structure under Scanning Electron Microscope (JEOL JSM-6710F) (a) Area 1 (b) Area 2

4.3.2 UV-Vis Spectrum

The unique colours of colloidal silver are due to a phenomenon named as plasmon absorbance. Figure 4.5 shows the UV-Vis Spectrum of the colloidal silver nanoparticles solution. The peak absorbance is at 380 nm. According to the simulations, this should give particles slightly bigger than 10 nm in diameter. At this wavelength, blue colour is absorbed. This describes the fact that the colloidal silver nanoparticles appear in yellow. The particle size in a solvent can be indicated by the wavelength of the plasmon absorption maximum in a

solvent (Meier et al., 2002). As observed with the FE-SEM investigations, the real values for the particles are in the range of 10 nm to 20 nm.

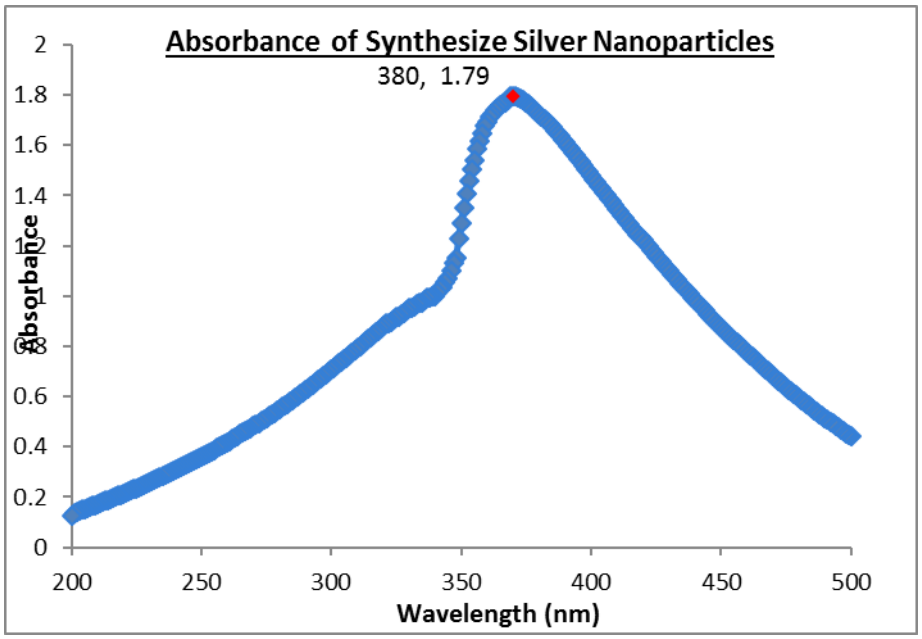

Figure 4.5: UV-Vis spectrum of Colloidal Silver nanoparticles solution

4.3.4 EDX Spectra

EDX Spectra were investigated on the colloidal silver nanoparticles samples and are shown in Figure 4.6. The gold originates from the Au grid and the same goes for palladium that from PD grid, but is also a very abundant material, as is the case for oxygen. This is to identify the presence of silver particles in the synthesized colloidal system from the reduction of silver nitrate by sodium borohydride. The result clearly shows that the presents of silver in the particles form during the synthesis.

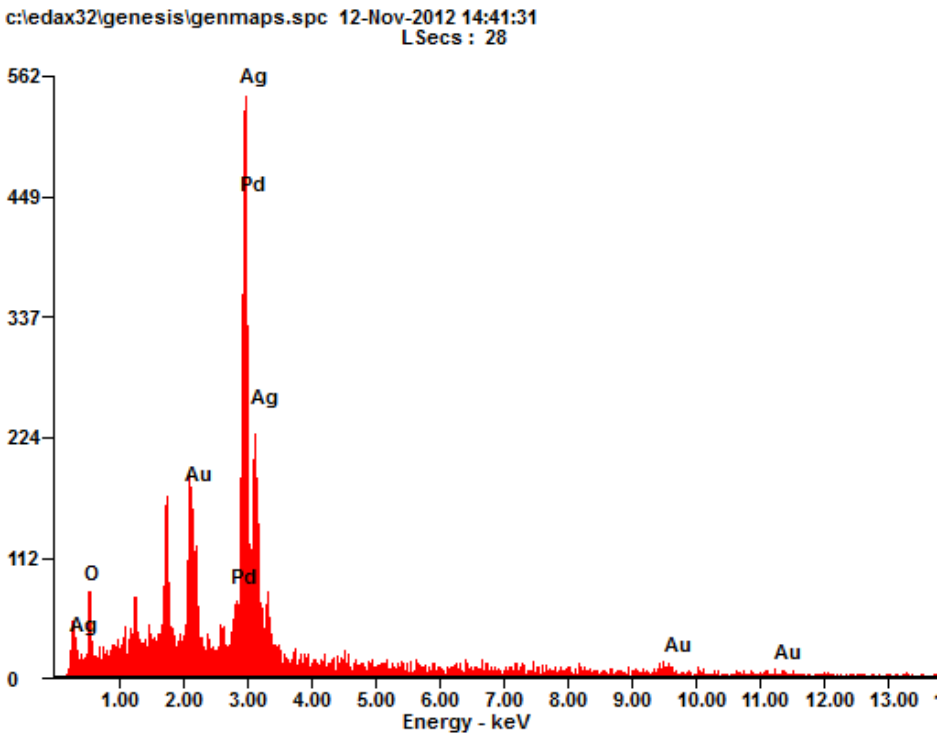

(a)

Element	Wt%	At%
OK	08.46	40.97
AuM	20.91	08.23
PdL	06.24	04.55
AgL	64.39	46.26
Matrix	Correction	ZAF

(b)

Figure 4.6: EDX spectra of colloidal synthesize silver nanoparticles (a) Absorbance of materials in the colloidal synthesize silver nanoparticles (b) Ratio of material present

CHAPTER 5

VISCOSITY CHARACTERISATION AND EMPIRICAL MODELLING

5.1 Introduction

This chapter shows the effects of weight fraction and size of fillers on the viscosity of ICAs. Power Law and Cross model are empirical models that help to quantify the viscosity of a material over a range of shear rates for ICAs and fit it into the experimental data. This study investigated the relationship of viscosity with different weight fraction and sizes of fillers of ICAs with three types of fillers that include silver flakes, commercial silver nanoparticles and synthesize silver nanoparticles. Lastly, a comparison between Cross model and Power Law Model will be done to identify which of it able to quantify the experimental data better.

5.2 Results and Discussion

5.2.1 Effect of size of the filler particles on viscosity of ICA pastes

Figure 5.1 (a) and (b) and showed the flow curves of formulated ICAs. As the shear rate increase, all the ICAs exhibit a reduction in viscosity. The reduction of viscosity clearly shows that all pastes are exhibiting shear thinning in nature

and their structure were breaking down as the suspension flocculation's is undergoing a destruction (Bao et al., 1998). Formulated ICAs with the same weight fraction of filler has an increase in viscosity as the particle size of filler is increasing. As the particles sizes increase, there are larger particles present in the same weight fraction of the formulated ICAs. The viscosity for the formulated ICAs that contain larger size of particles are high. As the fillers sizes increase, the packing stress will increase and lead to an increase is the viscosity (Haitham et al., 2011). Hence, the data show that due to the presence of larger particles is the ICAs, resulting a higher packing stress and hence, it increases the resistance to flow. Due to the filler with larger particles size will lead to a bigger aggregates suspension. This could result in a higher volume of particles and causing more immobilized liquid within the local structures (Behzadfar et al., 2009). Thus, resulting the viscosity of formulated ICAs with smaller filler particles is lower than ICAs with larger filler particles. Yet, as the shear rate increases, the viscosity drops for all the formulated ICAs. It shows that this effect is more noticeable with the increase of shear rate. This simply indicates that the inter-particles connections in the system are relatively weak and able to break down under high shear rate.

In this study, a comparison was mainly based on three silver nanoparticles with different particle size. First is commercial silver nanoparticles of 10 nm, commercial silver nanoparticles of 20 nm and synthesize silver nanoparticles with size in between 10 nm to 20 nm. The effect of silver nanoparticle size on the viscosity has been reported for ICAs with 0.8 weight fraction of filler load. At zero shear rate the viscosity of ICAs with silver nanoparticles 10 nm has the

lowest viscosity, 37900 Pa.s followed by 51100 Pa.s for silver nanoparticles 20 nm and highest viscosity is 15700 Pa.s for synthesize silver nanoparticles. As the particle size of the filler decrease, the viscosity decreases. This is due to the smaller particle size of filler have a lower effective volume of particle, thus the liquid in the local structures is more mobilized. Hence, viscosity is lower. Moreover, the resistivity of flow reduces, as the smaller particles did not agglomerate into bigger flocs in the system, then lead to the decrease of viscosity. We are able to observe that for ICAs formulated with synthesized silver nanoparticles has the highest viscosity. This is due to that it contains a range of size between 10 nm to 20 nm. This allows the high contact surface area of the particles to disperse better within the flux system. Therefore resulting a way more effective volume particle and lead to the highest resistivity of flow among all other samples (Behzadfar et al., 2009). Hence, it has the highest viscosity.

On the other hand, larger particle size filler will lead to higher packing stress and has a high effective volume of particles in the suspension (Haitham et al., 2011). Therefore, the overall viscosity of samples formulated with 20 nm silver nanoparticles is higher samples formulated with 10 nm silver nanoparticles.

5.2.2 Effect of weight fraction of filler on viscosity of ICA pastes

The filler content does have a significant effect on the viscosity and rheological properties of the formulated ICAs. Weight percent is usually used to specify the weight fraction. In an overall view, the viscosity of a disperse system decreases when the weight fraction of the filler content in it decreases. Figure 5.1 (a) and (b) clearly shows the impact of two different weight fraction of the suspended filler content on the viscosity of the ICAs with different types of filler that include silver flakes, commercial silver nanoparticles and synthesize silver nanoparticles with DGEBA resin.Samples 1 to 4 (S1 - S4) were formulated with 0.6 weight fraction of filler contents while samples 5 to 8 (S5 - S8) were formulated with 0.8 weight fraction of filler contents. The formulated ICAs with 0.8 weight fraction of filler content has a significant higher viscosity compare to the ICAs with 0.6 weight fraction of filler content. As the concentration of the filler increases, the inter-particle interactions increase as well. The bonding form in the suspension will be stronger and lead to an increase in the resistance to flow. Moreover, the high amount of filler will lead to a closer surface contact among each particle and collision occurs between the filler particles. ICAs at the weight fraction of 0.8, the amount of fillers are sufficient enough to have a closer contact among each particle, resulting in a higher degree of agglomeration among the fillers (Irfan and Kumar, 2008). This channel is actually a continuous linkage between all the filler and epoxy system. The result clearly indicates that ICAs with 0.8 of filler weight fraction have the best filler network.

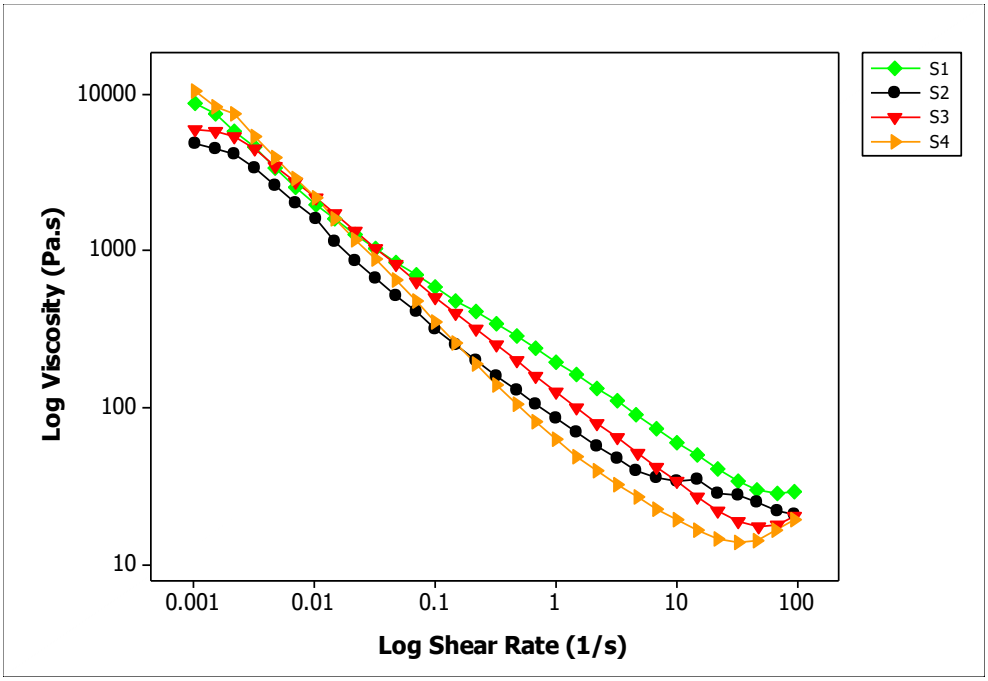

(a)

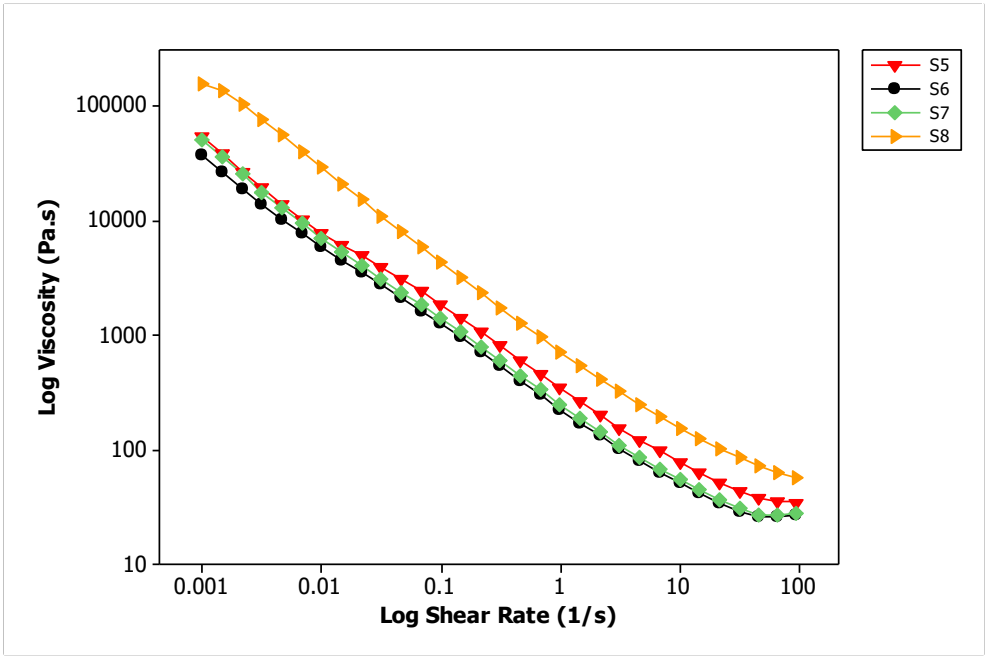

(b)

Figure 5.1: Flow curve of formulated samples (a) ICA pastes with 0.6 weight fraction of fillers contents, (b) ICA pastes with 0.8 weight fraction of fillers contents

5.2.3 Comparison between Power Law model and Cross model fitting to Experimental Data

Figure 5.2 shows the experimental viscosity data that were fitted to the Power Law and Cross model. We are able to observe that the Cross model curves exhibit a better fit compared to Power Law model curves for all samples. No doubt that both the models were designed to evaluate the shear thinning behaviour of a suspension, but the results show it has the best fit only on Cross Model. This may be due to the shear rate investigated are too wide and fall beyond the range of the Power Law model. In addition, it also could be due to the presence of three regions in all samples that can be easily captured by the Cross model. These three regions include Newtonian region, shear thinning region and the second Newtonian region. Results obtained associate well with previous studies (Durairaj et al., 2002) and also demonstrate that the formulated ICA exhibit the three regions when the samples are sheared from a low shear rate to a high shear rates. Thus, for a wider shear rate experiment, the Cross model provides a better experimental fit than the Power Law model even though both were able to evaluate the shear thinning behaviour of a suspension.

A further analysis was investigated along the fitted data, as presented in Table 5.1 and 5.2. The Power Law and Cross model were used to quantify the viscosity over shear rate profile for the shear-thinning formulated ICA and fit to the experimental data. In a Power Law model equation, if n, the power index, falls in between zero and one ($0<n<1$), this shows that the viscosity of the

sample being tested was exhibiting shear thinning behaviour (Evans and Beddow., 1987; McLelland et al., 1997; Bullard et al., 2009). From Table 5.1 and 5.2, we are able to observe that all the *n* values of samples S1 to S8 falls in between zero and one (S1=0.4881, S2=0.44756, S3=0.43461, S4=0.36059, S5=0.33629, S6=0.33215, S7=0.31194, S8=0.26663). Thus, the viscosities of all eight samples were undergoing shear thinning behaviour. In addition, for Cross model equation, *m*, the rate constant, measure the degree of dependence of viscosity on shear rate within the shear-thinning region (Koszkul and Nabialek, 2004). When *m*=0, this shows that the samples exhibit Newtonian behaviour. Whereas when m>0, this shows that the increasing of shear rate leads to a decrease on its viscosity. From Table 5.2, we are able to observe the rate constant, *m* values of all eight formulated ICA were more than zero, which also indicates that all samples have shear thinning behaviour (S1=0. 61726, S2=0. 73617, S3=0. 76487, S4=0. 72437, S5=0. 79863, S6=0. 83534, S7=0. 83835, S8=0. 85349).

R^2 is the correlation coefficient that exhibits the relationship between the shear rate and the viscosity. R^2 measured on how well the data correlated. The closer the R^2 value to one, the data will have a better correlation with the model (Mongomery et al., 2001). By comparing the correlation ratio, R^2 in Table 5.1 and 5.2, all the R^2 from Cross model is higher than R^2 from Power Law model for all formulated ICA. The highest R^2 value from the Cross model data is shown by S8 which is 0.997. All the R^2 value for all samples formulated are almost perfect linear relationships between viscosities and shear rates since all samples R^2 value is very close to one. No doubt for both the Power Law model

and Cross model are designed to evaluate suspension quality in this experiment, Cross model describe the results more precise than the Power Law model. This is due to the Power Law model does not provide more information on rheological properties of suspension in a wider range of shear rates if compare to the Cross model. In addition, the Power Law model does not describe the high-shear and low-shear rates constant-viscosity data of a fluid that exhibits shear-thinning. Therefore, the Power Law model does not fit well to the experimental data if compared with the Cross model (Rao, 2007).

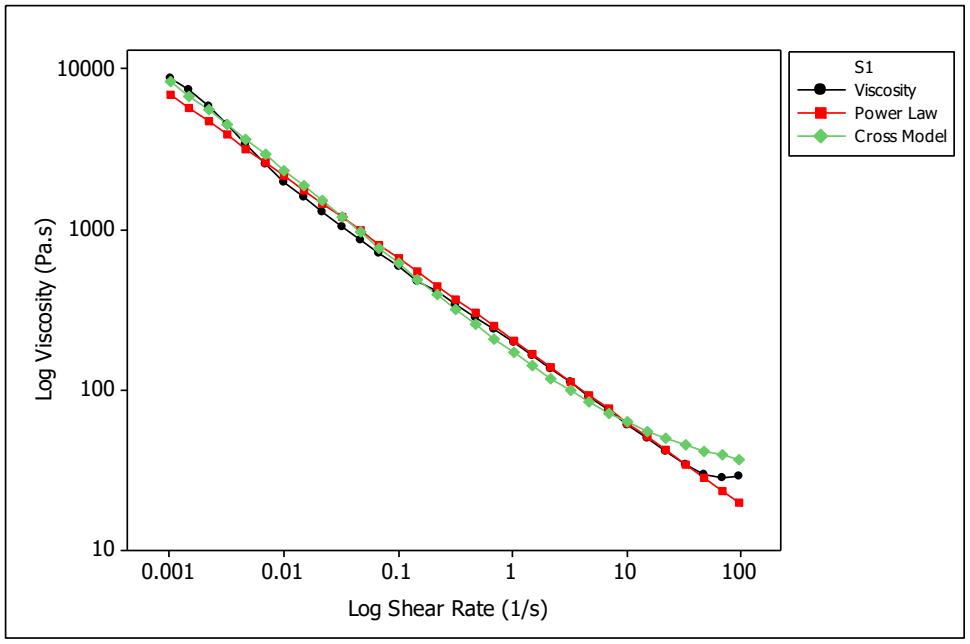

(a)

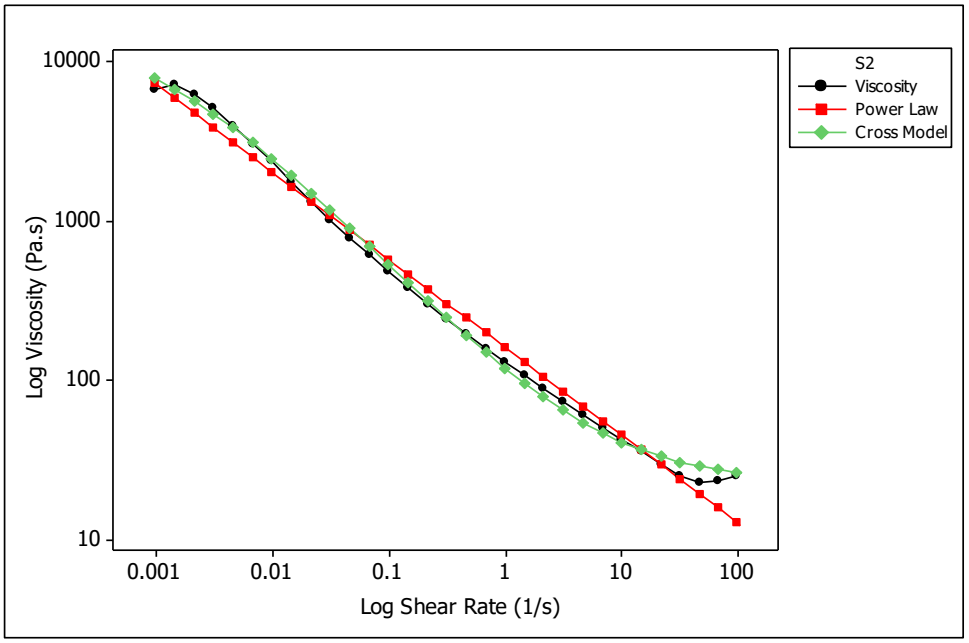
S2
Viscosity
Power Law
Cross Model
10000
1000
100
10
Log Viscosity (Pa.s)
0.001
0.01
0.1
1
10
100
Log Shear Rate (1/s)

(b)

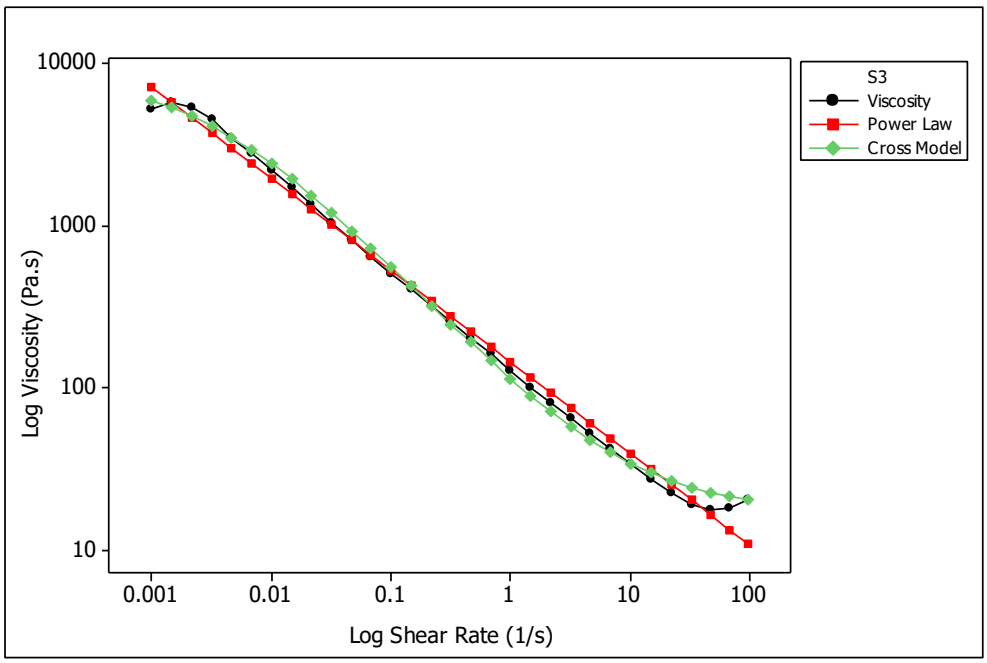
S3
Viscosity
Power Law
Cross Model
10000
1000
100
10
Log Viscosity (Pa.s)
0.001
0.01
0.1
1
10
100
Log Shear Rate (1/s)

(c)

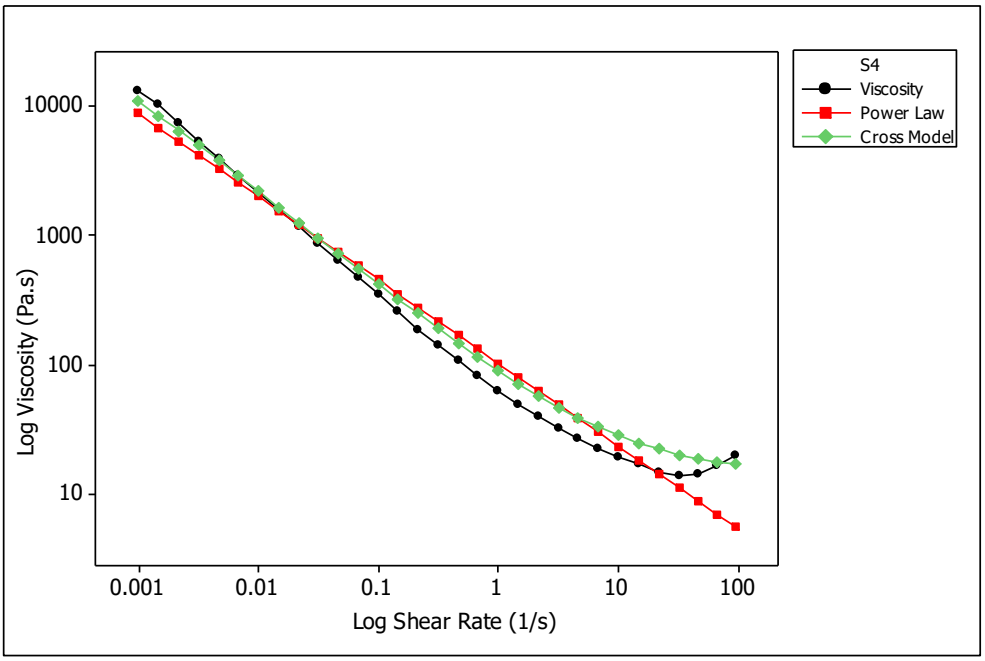
S4
Viscosity
Power Law
Cross Model
10000
1000
100
10
Log Viscosity (Pa.s)
0.001
0.01
0.1
1
10
100
Log Shear Rate (1/s)

(d)

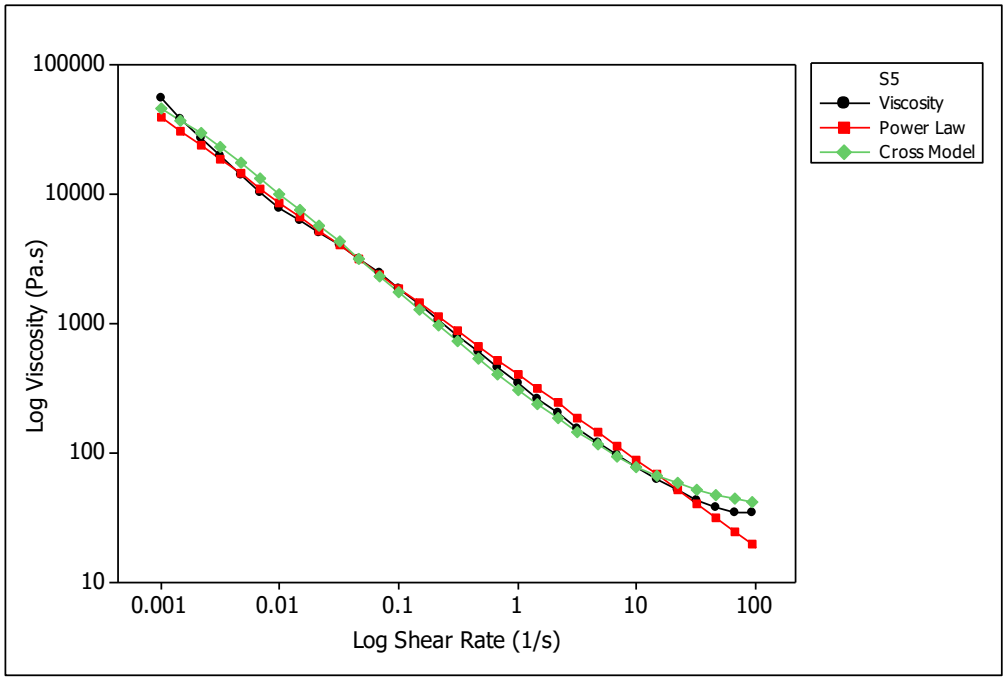
S5
Viscosity
Power Law
Cross Model
100000
10000
1000
100
10
Log Viscosity (Pa.s)
0.001
0.01
0.1
1
10
100
Log Shear Rate (1/s)

(e)

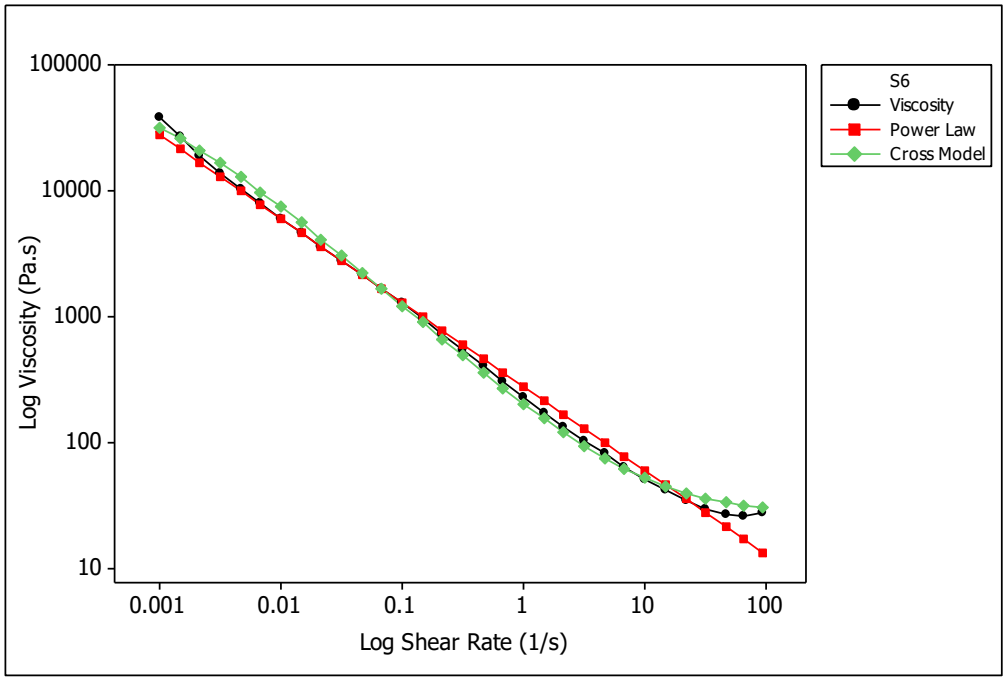
S6
Viscosity
Power Law
Cross Model
Log Viscosity (Pa.s)
100000
10000
1000
100
10
0.001
0.01
0.1
1
10
100
Log Shear Rate (1/s)

(f)

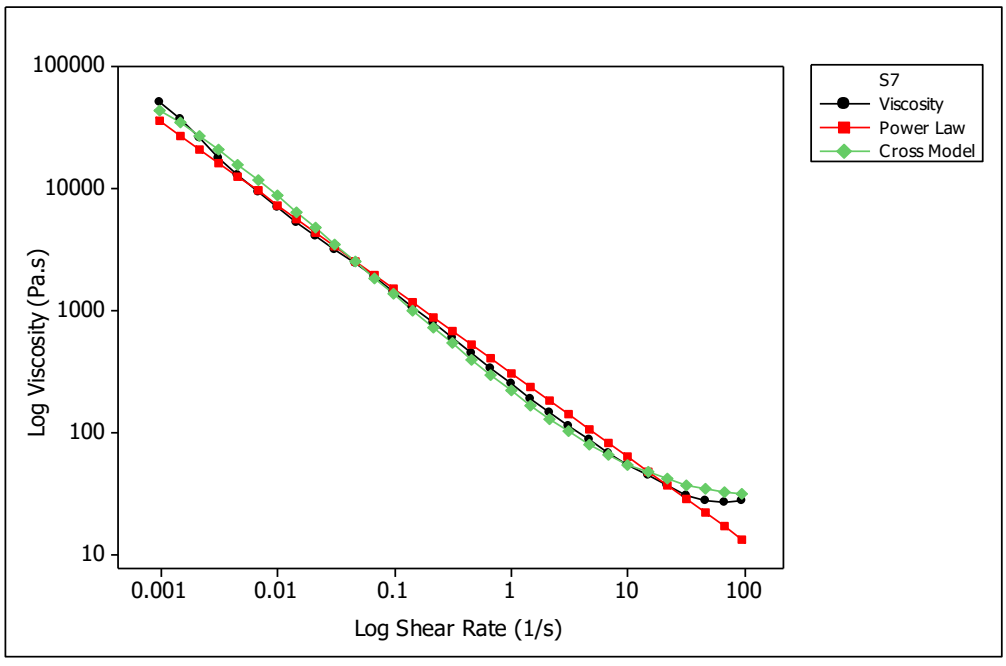
S7
Viscosity
Power Law
Cross Model
Log Viscosity (Pa.s)
100000
10000
1000
100
10
0.001
0.01
0.1
1
10
100
Log Shear Rate (1/s)

(g)

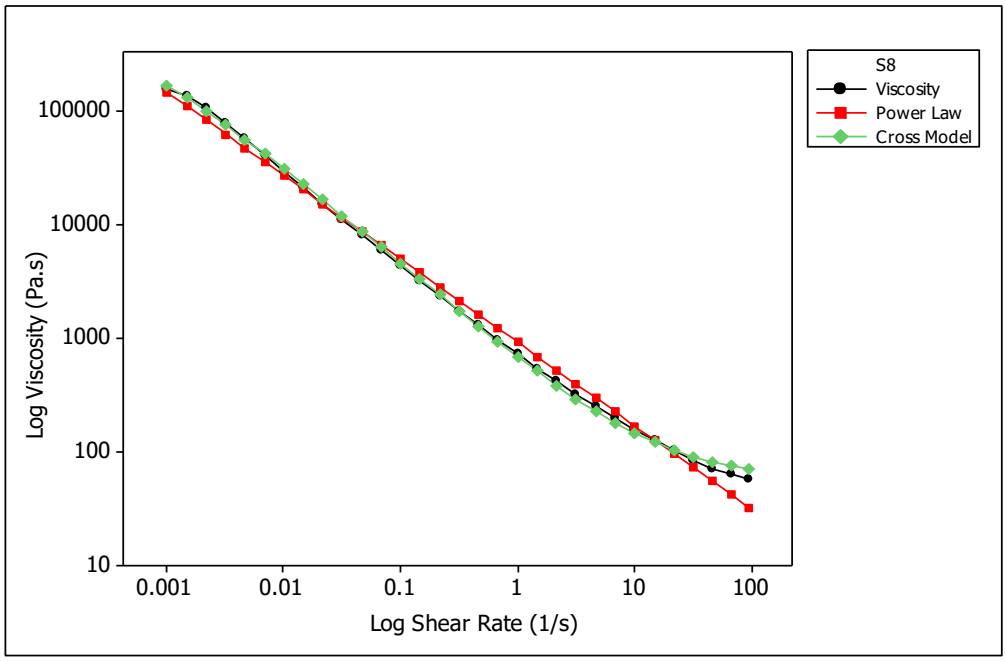

(h)

Figure 5.2: Flow curve of formulated sample (a) S1, (b) S2, (c) S3, (d) S4, (e) S5, (f) S6, (g) S7, and (h) S8

Table 5.1: Variables Collected in Power Law model

Samples	Consistency coefficient, *K* (Pa.s)	Power Law indexes, *n*	Correlation ratio, R^2
S1	204.39	0.4881	0.979
S2	161.36	0.44756	0.955
S3	143.13	0.43461	0.937
S4	101.33	0.36059	0.979
S5	405.99	0.33629	0.966
S6	277.67	0.33215	0.962
S7	307.06	0.31194	0.974
S8	918.16	0.26663	0.983

Table 5.2: Variables Collected in Cross model

Samples	Infinite shear viscosity, (Pa.s)	Zero shear viscosity, (Pa.s)	Rate constant, *m*	Correlation ratio, R^2
S1	28.469	44,359	0.61726	0.994
S2	23.127	15,638	0.73617	0.983
S3	17.383	8,473.3	0.76487	0.986
S4	13.833	133,820	0.72437	0.996
S5	34.791	138,550	0.79863	0.984
S6	25.881	69314	0.83534	0.988
S7	26.599	140,040	0.83835	0.986
S8	57.200	591,510	0.85349	0.997

CHAPTER 6

VISCOELASTIC STUDIES

6.1 Introduction

This chapter presents the study on the viscoelastic behaviour of formulated ICAs formulated with different sizes of silver nanoparticles. The chapter contains three sections. The first section describes the viscoelastic behaviour of paste. The second section shows the results of the oscillatory stress sweep test. The last section provides the summary of the experimental study.

6.2 Results and Discussion

6.2.1 Study of paste structures within the linear viscoelastic region (LVER)

The region where maximum deformation can be applied to the sample without destroying its structure is the linear viscoelastic region. It is in this region, all the particles are close contact with each other and able to recover elastically to any applied strain or stress. Consequently, the suspension now acts as a solid and the structure remains intact as is it. By increasing strain or stress more than this region, the structure of the material is progressively demolished. Within the linear viscoelastic region, the loss modulus, G" and storage modulus, G', which represents the liquid and solid characteristics are able to deliver an

insight into the paste behaviour before the structure of the paste begin to breakdown.

The linear viscoelastic region (LVER) must first be defined before proceed to any detailed dynamic measurement to the sample's microstructure. LVER can be determined by performing the amplitude stress sweep test. The stability of a suspension can be studied by identifying the LVER. To be precise, the length of the storage modulus (G') that falls within LVER provides a better understanding of the stability of the sample's structure, which is associated to its elasticity. A sample that is well-dispersed and has a stable system will have a long LVER. The oscillatory stress sweep results revealed that the linear viscoelastic region for all 0.8 weight fraction of formulated ICAs were approximately below 0.02 Pa. On the other hand, all 0.6 weight fraction of formulated ICAs were below 0.05 Pa. This indicates that both of the LVER for 0.8 weight fraction of ICAs and 0.6 weight fraction of ICAs lies within small stress range. Thus, when the shear stresses are low, all the ICAs exhibit a dominant elastic behaviour (G'>G").

The oscillatory stress sweep tests results for all the samples are shown in Figure 6.1. Based on Figure 6.1 (a) and (b), 0.6 and 0.8 the weight fraction of all formulations of epoxy and fillers are represented as sample S1, S2, S3, S4, S5, S6, S7, and S8 exhibits a dominant elastic behaviour as the elastic modulus is higher than the viscous modulus. The elastic properties, G' increase significantly with the increase of filler content in a suspension (Rajinder 2005). As the concentration of filler increase, the amount of particles in the

suspension increases too. This will lead to an increase of contact surface area and the collision within each particle of the filler. Therefore, 0.8 weight fraction of ICAs samples includes S5, S6, S7, and S8 have fillers that are satisfactory enough to contact closure within each particle, lead to a higher degree of fillers agglomeration (Irfan and Kumar, 2008). As a result, 0.8 weight fraction of ICAs samples have a significantly higher value of G' compare to 0.6 weight fraction of ICAs samples. This channel is essentially a continuous linkage between all the filler and epoxy system. Figure 6.1 (c) shows the viscosity for pure DGEBA when shear is applied. The G' and G" clearly shows that pure DGEBA is a Newtonian fluid as they nearly remain constant even when shear is applied from low to high shear.

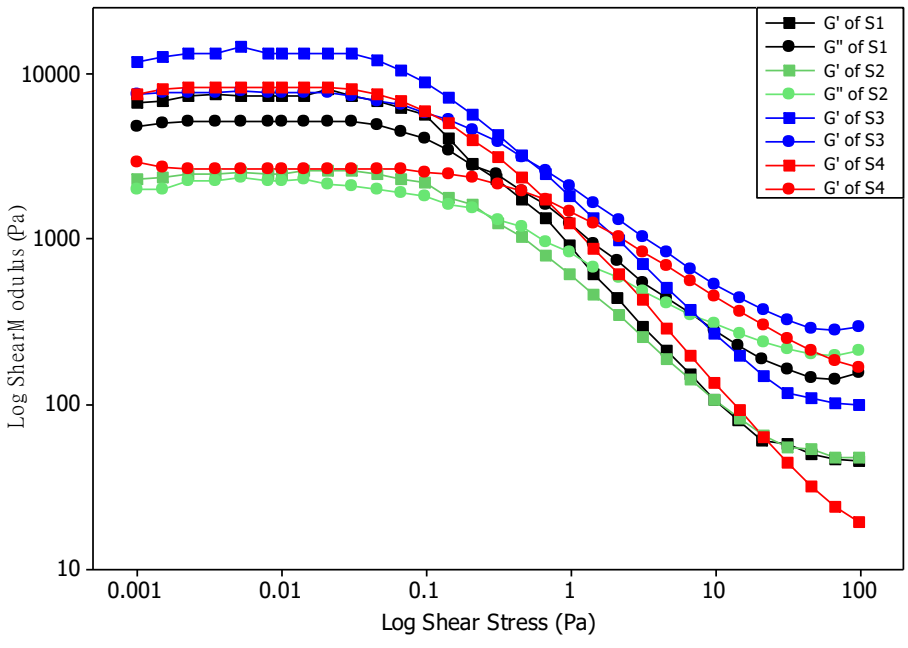

(a)

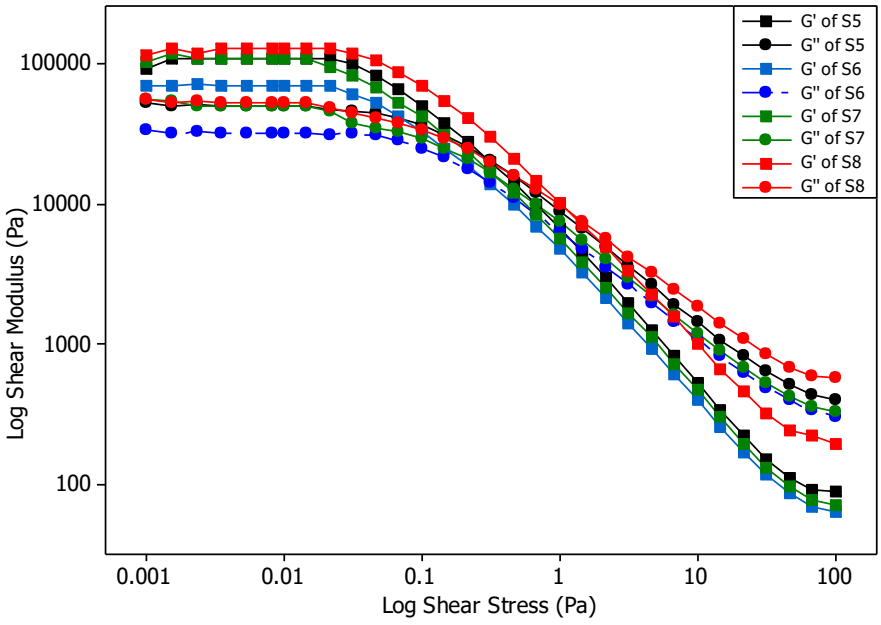

(b)

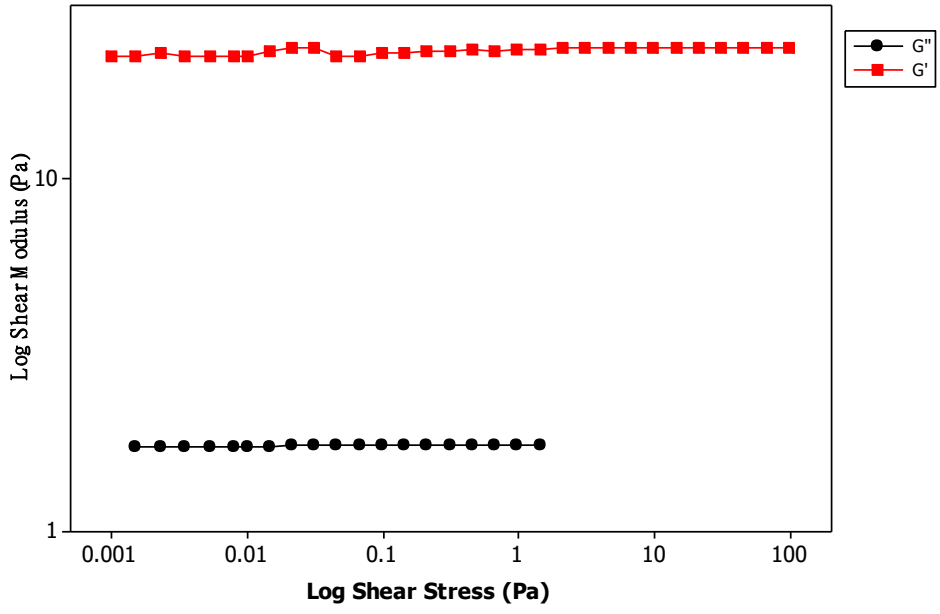

(c)

Figure 6.1: Oscillatory stress sweep for (a) ICA pastes with 0.6 weight fraction of fillers contents, (b) ICA pastes with 0.8 weight fraction of fillers contents, (c) Pure DGEBA Resin

A further analysis of the elastic behaviour of paste was investigated by calculating the ratio of viscous properties to elastic properties (G"/G') within the LVER. The calculated data are shown in Table 6.1. The ratio G"/G' provides an indication of interaction strength within the internal structure of a flux system. A material that is elastic in nature will have a lower G"/G' ratio (Durairaj et al., 2008). From the results observed from Table 6.1, all the samples have a ratio that is lower than one. Thus, all formulated ICAs are elastic in nature. ICAs formulated with 0.8 weight fractions have the G"/G' value in the range of 0.42 to 0.62. On the other hand, ICAs formulated with 0.6 weight fractions have the G"/G' value in the range of 0.51 to 0.87. Overall samples with a 0.8 weight fraction of filler contents (S5, S6, S7, and S8) has a lower G"/G' ratio than the others samples with a 0.6 weight fraction of filler contents (S1, S2, S3, and S4). The lower G"/G' ratio shows that the formulated ICA is very cohesive or tacky. Hence, samples formulated with 0.8 weight fractions are more elastic than samples formulated with 0.6 weight fraction. It is due to higher filler content in the samples and eventually lead to a more cohesive paste. This could cause a poorer paste withdrawal during the aperture emptying process. Factors such as the epoxy-filler, inter particle bonding and particle sizes may influence the cohesive nature and solid characteristic of an ICA. A visual observation of the formulated ICAs in Figure 6.2 clearly shows that the formulated ICAs with 0.8 weight fraction stay intact and tacky. However, Figure 6.3 presents that the formulated ICAs with 0.6 weight fraction is not as intact and tacky as 0.8 weight fraction.

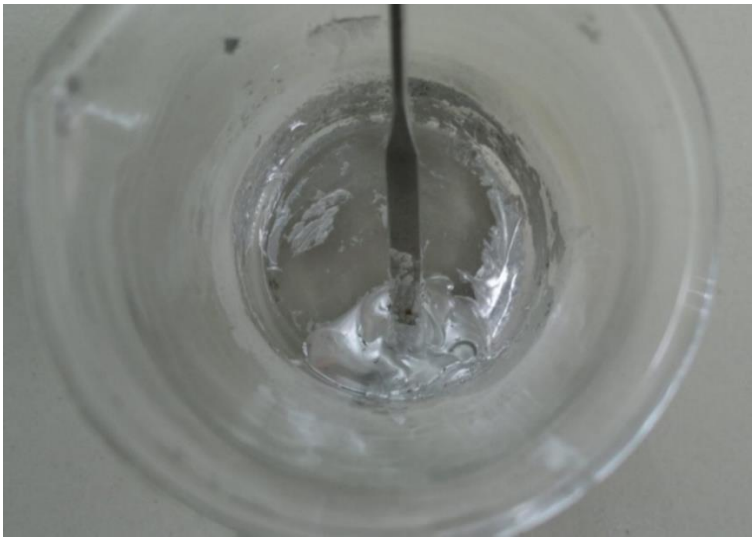

Figure 6.2: ICAs formulated with DGEBA resin and 0.8 weight fraction of filler contents

Figure 6.3: ICAs formulated with DGEBA resin and 0.6 weight fraction of filler contents

Table 6.1: Summary of the oscillatory stress sweep parameter within the LVER for formulated ICAs of 0.6 and 0.8 weight fraction of fillers.

Sample	G' (Pa)	G" (Pa)	G"/G'
S1 (0.4 DGEBA/0.6 Silver Flakes)	6700	4840	0.72
S2 (0.4 DGEBA/0.6 Silver Flakes + Silver Nanoparticles 10nm)	2300	1990	0.87
S3 (0.4 DGEBA/0.6 Silver Flakes + Silver Nanoparticles 20nm)	11990	7650	0.64
S4 (0.4 DGEBA/0.6 Silver Flakes + Synthesize Silver Nanoparticles)	7570	3860	0.51
S5 (0.2 DGEBA/0.8 Silver Flakes)	91500	52000	0.57
S6 (0.2 DGEBA/0.8 Silver Flakes + Silver Nanoparticles 10nm)	69200	33900	0.49
S7 (0.2 DGEBA/0.8 Silver Flakes + Silver Nanoparticles 20nm)	101500	55400	0.55
S8 (0.2 DGEBA/0.8 Silver Flakes + Synthesize Silver Nanoparticles)	114000	47800	0.42

Both ICAs formulated with silver nanoparticles 10nm (S2 and S6) have a higher G"/G' ratio than ICAs formulated with silver nanoparticles 20 nm (S3 and S7). This may be due to the large particles agglomerating into larger flocs and resulting in a denser paste and therefore, exhibiting more solid like behaviour. In brief, this shows that the increase in the size of the filler particle leads to an increase in cohesiveness of the paste. ICAs formulated with synthesized silver nanoparticles have the lowest G"/G' ratio, which is 0.51 for S4 and 0.42 for S8. This could be due to the synthesize silver nanoparticles have a size range between 10 nm to 20 nm that allow the particles to disperse well enough in the flux system, then lead to a more effective volume of particles packing in the system. Hence, these two samples are most elastic

among other formulation. For sample S4, 0.6-silver flakes + synthesize silver nanoparticles with 0.4-DGEBA system has the G"/G' ratio of 0.51 which is same as the G"/G' ratio of S4, 0.8-silver flakes + silver nanoparticles 20 nm with the 0.2-DGEBA system. This indicates that both of these formulated ICAs share the same viscoelastic properties.

6.2.2 Correlation of stress at G'= G'' to the paste cohesiveness

The stress at G'= G" which is the yield at the highest shear stress value in an oscillatory stress sweep curve at the point where the isotropic conductive adhesive is yet to start flowing. It is the point where the internal forces of the rheological network in the solder paste are lower than the external forces of gravity or squeegee applied to it (Lapasin et al., 1997). The formulated ICAs has an elastic behaviours for stress below its yield point. It does not deform and behaves towards a solid-like substance. It does not separate nor slump during a stencil printing process. After the stress passed the yield point, the ICAs behaviour will have a transition from the solid-like to liquid-like behaviour (Durairaj et al., 2009). Table 6.2 showed the measured yield point for 0.8 weight fraction and 0.6 weight fraction of the epoxy-filler system. The results clearly show that ICAs formulated with synthesized silver nanoparticles has the highest yield point among others where S4 has a yield point of 0.655 Pa and 1.107 Pa for S8. Yield point could also act as an indicator for accessing the cohesiveness of the formulated ICAs. It is a significant characteristic because the ability for a paste to flow from the stencil aperture depends on the liquid

behaviour of the paste. As the yield point value increase, the paste can only gradually change solid-like to liquid-like behaviour under a large amount of stress. Meanwhile, it also shows that the system has a stronger rheological network and low tendency for sedimentation of the formulate ICAs particles. This indicates that addition of synthesized silver nanoparticles in the paste formulation delay the structural breakdown to a higher stress. In addition, the increase of cohesiveness and tackiness characteristic of paste formulated with synthesized silver nanoparticles able to reduce the chances of sedimentation to occur. Nevertheless, high cohesiveness may affect the flow of the paste into the apertures and lead to poorer paste release from apertures in a stencil printing process.

Table 6.2: Yield Point, G' = G'' formulated ICAs of 0.6 and 0.8 weight fraction of fillers

Sample	Stress at G' = G"
S1 (0.4 DGEBA/0.6 Silver Flakes)	0.295
S2 (0.4 DGEBA/0.6 Silver Flakes + Silver Nanoparticles 10nm)	0.219
S3 (0.4 DGEBA/0.6 Silver Flakes + Silver Nanoparticles 20nm)	0.348
S4 (0.4 DGEBA/0.6 Silver Flakes + Synthesize Silver Nanoparticles)	0.655
S5 (0.2 DGEBA/0.8 Silver Flakes)	0.308
S6 (0.2 DGEBA/0.8 Silver Flakes + Silver Nanoparticles 10nm)	0.318
S7 (0.2 DGEBA/0.8 Silver Flakes + Silver Nanoparticles 20nm)	0.337
S8 (0.2 DGEBA/0.8 Silver Flakes + Synthesize Silver Nanoparticles)	1.107

6.2.3 Correlation of phase angle to quality of pastes formulation

A suspension that has an elastic (solid) behaviour consists of a phase angle (δ) that is closer to 0˚. Whereas a suspension that has a viscous (liquid) behaviour consist a phase angle that is closer to 90˚ (Ferguson and Kemblowski, 1991). Phase angles between 0˚ and 90˚ will exhibit a viscoelastic behaviour (Bao et al., 1998 and Lapasin et al., 1997). The phase angle could provide better understanding of the transition from solid-like to liquid-like behaviour of a

suspension. In brief, a paste with a lower phase angle may be very tacky and a paste that has a high phase angle may easily slump during the printing process.

All phase angle values are shown in Table 6.3. All phase angle values for the formulated ICAs lie between 0˚ and 90˚. The oscillatory results clearly show that all pastes are viscoelastic in nature, which in agreement with previous research (Bao et al., 1998; Lapasin et al., 1997; Durairaj et al., 2008). For all 8 samples, S4 and S8 that are formulated with synthesized silver nanoparticles have the lowest phase angle which is 34.6 and 30.2. This indicates that the adding of synthesized silver nanoparticles into the formulation will result in cohesive paste. This could be due to that synthesize silver nanoparticles has a size range of 10 nm to 20 nm. This will allow each particle to fill in the gap in between that will reduce flocs and lead to a stronger attraction among each particle in the system. Hence, both S4 and S8 are more cohesive pastes than the others. In addition, for all samples with 0.8 weight fraction has a higher phase angle than the others samples. This could be due to the high amount of filler content and lead to a stronger particle-particle interactions (Rajinder 2005). As mentioned earlier, as the particles size increase, the paste tackiness and cohesiveness will increase due to the particles agglomerate into larger flocs and increase the resistivity of flow (Irfan and Kamar, 2008). Thus, the data in Table 6.3 shows that S3 and S7 has a lower phase angle if compare to S2 and S8. In fact, researchers and engineers would be able to formulate a material that has minimal separation during and after the printing process with the help of the phase angle reading of the paste. The phase angle readings collected from the

test is able to help engineer to evaluate the overall quality of dispersion of a batch production of paste to another batch of paste.

Table 6.3: Phase angle for formulated ICAs of 0.6 and 0.8 weight fraction of fillers.

Sample	Phase angle, (δ)
S1 (0.4 DGEBA/0.6 Silver Flakes)	48.8
S2 (0.4 DGEBA/0.6 Silver Flakes + Silver Nanoparticles 10nm)	46.2
S3 (0.4 DGEBA/0.6 Silver Flakes + Silver Nanoparticles 20nm)	45.6
S4 (0.4 DGEBA/0.6 Silver Flakes + Synthesize Silver Nanoparticles)	34.6
S5 (0.2 DGEBA/0.8 Silver Flakes)	46.4
S6 (0.2 DGEBA/0.8 Silver Flakes + Silver Nanoparticles 10nm)	42.8
S7 (0.2 DGEBA/0.8 Silver Flakes + Silver Nanoparticles 20nm)	41.4
S8 (0.2 DGEBA/0.8 Silver Flakes + Synthesize Silver Nanoparticles)	30.2

CHAPTER 7

THIXOTROPIC STUDIES

7.1 Introduction

This chapter presents the thixotropic studies of the ICAs formulated with different sizes of silver nanoparticles. The chapter contains three sections. The first section describes the thixotropic behaviour for formulated ICA pastes with the hysteresis loop test. Second section discusses the result obtain via steady shear rate test to relate with the results from the hysteresis loop test. Lastly, the recovery percentages of all formulated ICAs are correlated with the paste thixotropic behaviour.

7.2 Results and discussion

7.2.1 Thixotropic properties of formulated ICA pastes

Figure 7.1 presents the hysteresis loop for all formulated ICAs. All ICAs was applied with high shear rate, 10 sec^{-1} with time and recover back to the initial shear rate, 0.01 sec^{-1}. The total time interval was 240 seconds. The influence of increasing shear rate on the viscosity for the formulated ICAs was being studied. All samples that have a decrease in viscosity clearly show that they are

shear thinning in nature and the ICAs structure were disrupted as this is the results of destruction of flocculation's in the suspensions (Durairaj et al., 2009). All eight samples show a hysteresis area when the hysteresis loop test is performed. It is the area between the up-curve and down-curve that is observed. The area between the up curve and down curve shows that the paste is thixotropic in nature, which have been proven in previous studies on isotropic conductive pastes (Bao et al., 1998; Durairaj et al., 2009). In brief, all eight samples in this study are thixotropic suspensions. The enclosed area within the hysteresis loop represents the extent of the structural breakdown within the sample when shear is applied (Durairaj et al., 2009).

The concentration of filler has a significant impact on the viscosity and rheological properties of ICAs (Bullard et al., 2009). In brief, the viscosity of a disperse suspension increase with the increase of weight fraction of the suspended filler content. The viscosity will increase completely with increasing the filler content. The increase of the filler content leads to the increase of inter-particle interactions, hence, resulting a very strong bonding within particles as concentration becomes higher and higher. Figure 7.1 (a) and (b) shows the hysteresis loop for ICAs formulated with 0.6 weight fraction and 0.8 weight fraction. By comparing both ICAs with weight fraction 0.6 and 0.8, we are able to observe that all ICAs formulated with 0.6 weight fraction of filler contents has a larger area within the hysteresis loop. This evidently shows that these samples undergo a larger structural break down. This is due to the bonding and interactions within the particles in the suspension are weak. The small hysteresis loop area for all ICAs with 0.8 weight fractions corresponds to

a thixotropic state where the inter particle bonding are strong enough resulting the particles to have a quick rearrangement within the structure after shear was removed. For ICAs with 0.8 weight fraction, the filler content is adequate enough to have closer contact, leads to a higher degree of fillers agglomeration (Irfan and Kumar, 2008). Thus, this channel is essentially a continuous linkage between all the filler and epoxy system.

Figure 7.1 (a) and (b) also shows the effect of increasing the concentration filler content on relative viscosities of the ICAs with different types of filler includes silver flakes, commercial silver nanoparticles and synthesize silver nanoparticles. Figure 7.2 presents that the viscosities of pure resins DGEBA that are almost independent of shear rate. As explained earlier, the region between the up curve and down curve in the hysteresis loop is an indication of the ICAs thixotropic behaviour, whereas the size of the enclosed area within the loop represents the extent of the structural breakdown in the ICAs when shear is applied (Mewis and Wagner, 2009). Sample S4 and S8 show the highest degree of thixotropy in each respective group of formulated weight fraction as they have the largest hysteresis loop area than all other ICAs. The large area within the hysteresis loop in both samples shows that they undergo a large structural breakdown when shear was applied. Comparison was made on two fillers of different particle size, which are commercial silver nanoparticles of 10 nm and commercial silver nanoparticles of 20 nm. As stated earlier, as the fillers sizes increase, the packing stress will increase and lead to an increase in the viscosity (Haitham et al., 2011). Therefore the viscosity for both S3 and S7 that formulated with commercial silver nanoparticles of 20 nm has a higher

viscosity after shear is applied than both S2 and S6 that formulated with commercial silver nanoparticles of 10 nm.

Sample S4 and S8 are formulated with synthesized silver nanoparticles. This indicates that adding synthesize silver nanoparticles into the formulation of ICAs will cause the suspension to have a larger structural breakdown as shear is applied. Hence, these two samples have a weak structural bonding that can be easily broken down by applying shear rate. Yet, the results show the recovery of the paste after large structural breakdown is better than the other samples as the recovered viscosity is very close to the initial viscosity before the shear was applied. This due to that even the attraction between the particles in sample S4 and S8 can be broken down easily, but the bonding also able to rebuild quickly and lead to a better recovery even after shear rate is removed. Thus, samples formulated with synthesized silver nanoparticles are said to have a strong thixotropic behaviour. To support this justification, the steady shear rate test was carried out.

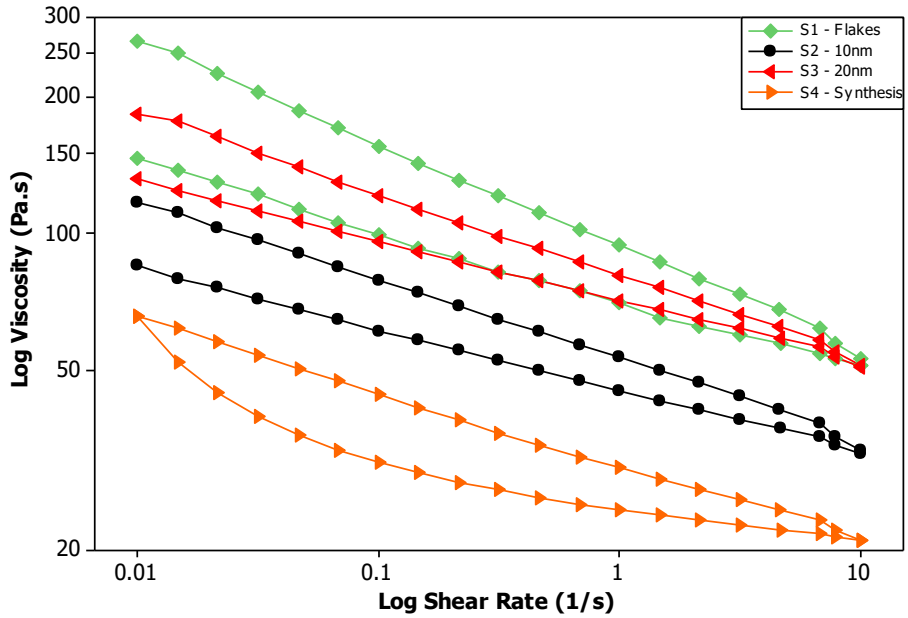

(a)

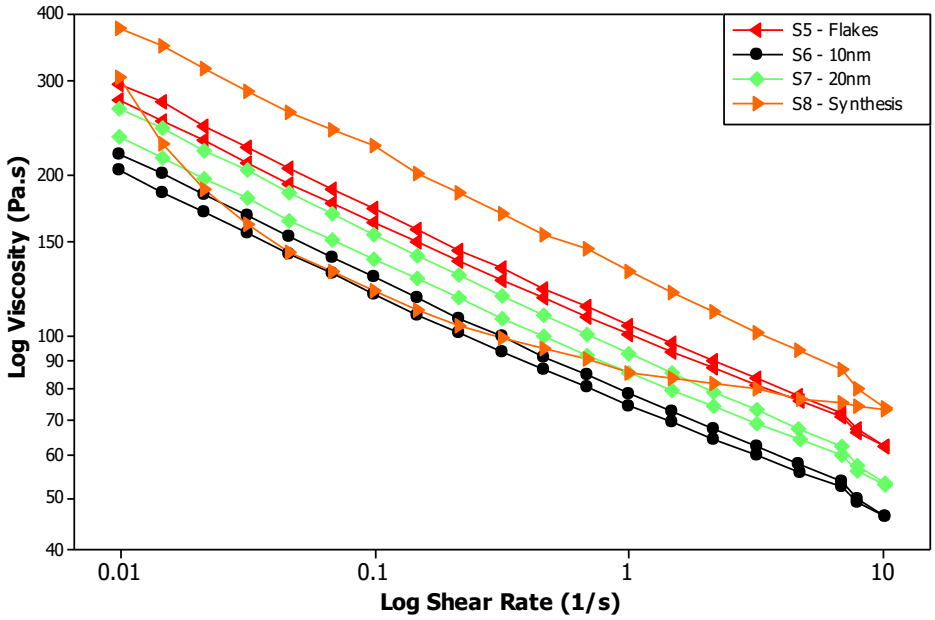

(b)

Figure 7.1: Hysteresis loop for (a) ICA pastes with 0.6 weight fraction of fillers contents, (b) ICA pastes with 0.8 weight fraction of fillers contents

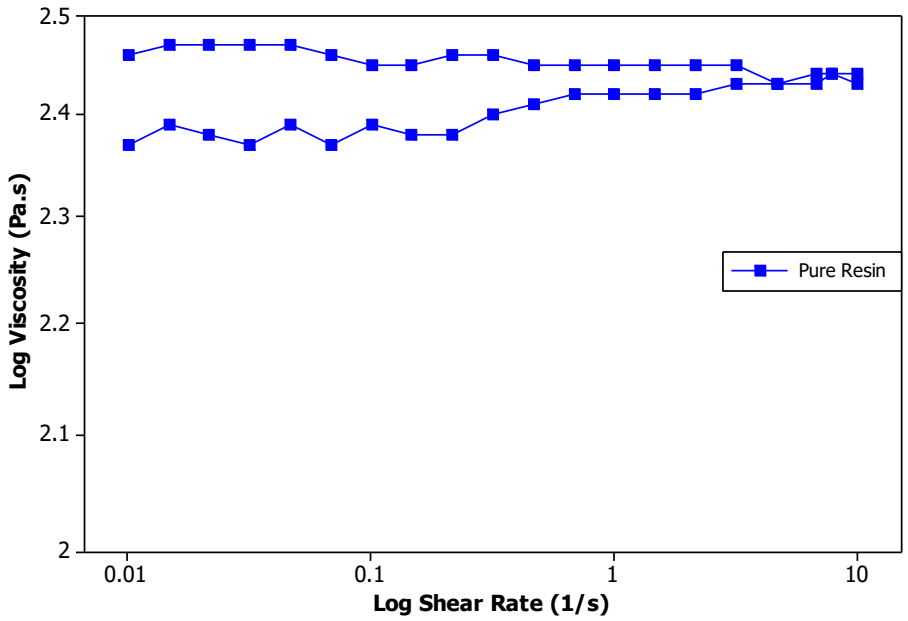

Figure 7.2: Hysteresis loop for Pure DGEBA Resin

Figures 7.3 (a) and (b) present the steady shear rate plot for all formulated ICA samples. Viscosities of all formulates ICA are gradually increase after the shear is removed (Mewis and Wagner, 2009). It is noticeable that all formulated ICAs show very good recoveries after the removal of shear. When high shear is applied, it can be observed that the S4 has a larger structural break down as the viscosity drops significantly lower than the others. Yet, the recovered viscosity is relatively close to initial viscosity before shear is applied. Sample S3 has a slightly scattered recovery viscosity; this suggests that the paste mixture is not well dispersed resulting in a poorer stability compared to other samples.

Figure 7.4 presents that the viscosities of pure resins DGEBA that are almost independent of shear rate. This clearly shows that DGEBA is a Newtonian Fluid as it is independent of shear rate. As mentioned earlier in Chapter 2,

Newtonian fluid is independent of the forces applied to it. This indicates that the fluid continues to flow, regardless of any forces applied to it (Larson, 1999; Mewis and Wagner, 2009). Thus, the structure of pure DGEBA resin was not being interrupted even shear rate is applied on it and there would be no recovery showed in the steady state rate plot.

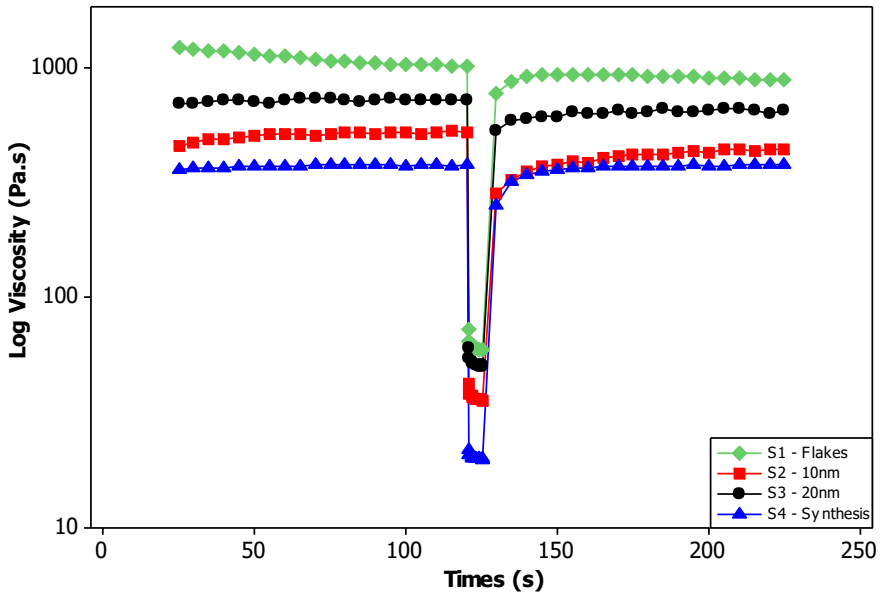

(a)

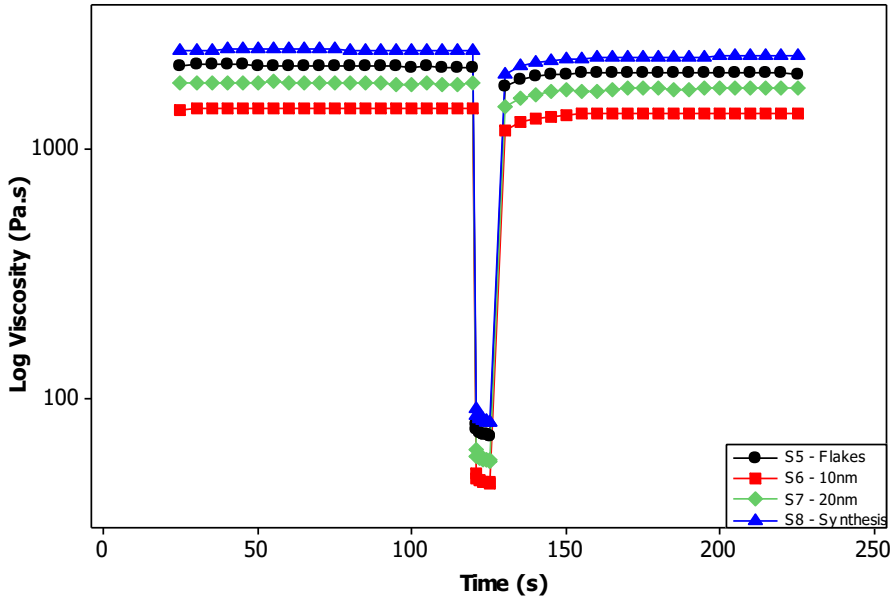

(b)

Figure 7.3: Steady Shear Rate Test for (a) ICA pastes with 0.6 weight fraction of fillers contents, (b) ICA pastes with 0.8 weight fraction of fillers contents

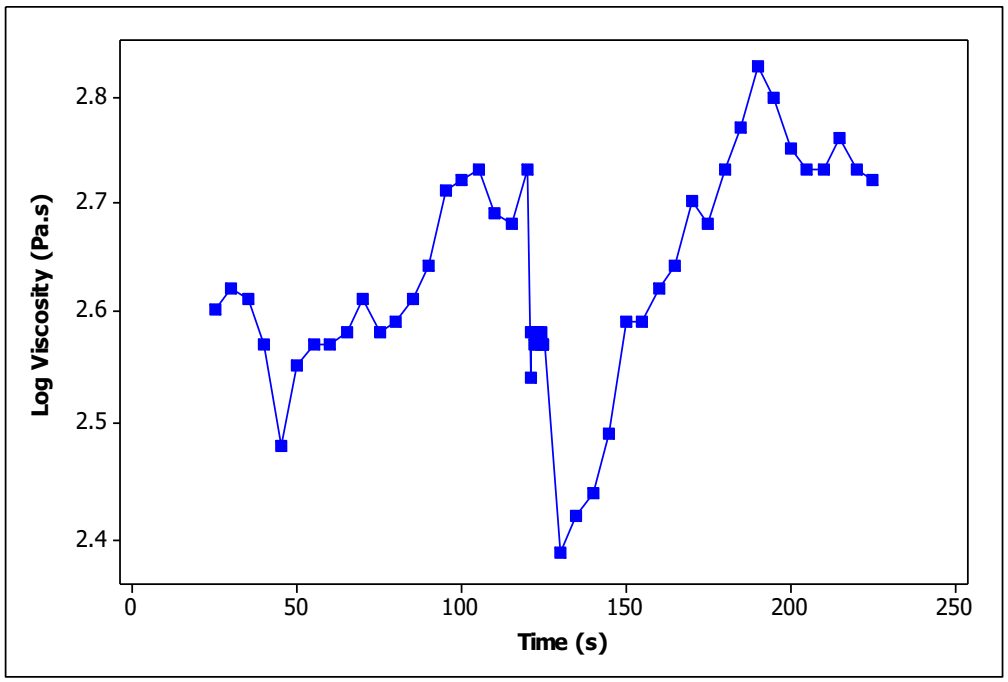

Figure 7.4: Steady Shear Rate Test for Pure DGEBA Resin

7.2.2 Correlation of recovery percentage of ICAs to its thixotropic behaviour

The recovery percentage between the structural breakdown or shear interval and build-up or recovery interval in a steady shear rate plot is measured using the equation showed in (Lapasin et al., 1997). Table 7.1 shows the recovery percentage for all samples. A sample that has a high recovery percentage exhibit a good thixotropic behaviour. By comparing the recovery percentage between formulated ICAs with 0.6 weight fraction and 0.8 weight fraction, the overall percentage of recovery is higher for ICAs with 0.8 weight fraction. The recovery percentage for the S4 is 92.40, which is higher than S1, 84.50, S2, 80.03 and S3, 87.67. Meanwhile, the recovery percentage for S8 is 95.54 which is also higher than S5, 92.39, S6, 92.21 and S7, 93.46. The results show that the formulated ICAs with 0.8 weight fraction have higher elastic behaviour opposed to those with 0.6 weight fraction. This indicates that they have a good recovery after the shear is removed. It matched the result obtain from the hysteresis loop where the inter particle bonding is stronger, hence lead to a quick rearrangement within the structure after the removal of shear. The formulated ICAs either with 0.8 weight fraction or 0.6 weight fraction, samples formulate with synthesized silver nanoparticles showed the highest percentage of recovery after removal of shear. This calculation of recovery percentage matches the recovery curve in hysteresis loop where even after a large structural breakdown, both of it still able to recover to a viscosity that is very close to initial viscosity before shear was applied. This is due to that it contains a range of size between 10 nm to 20 nm. This allows the high contact surface

area of the particles to disperse better within the flux system. A system that is well dispersed will lead to a high stability suspension (Barnes, 1989). Thus, even attraction between the particles in sample S4 and S8 can be broken down easily, but the bonding also able to rebuild quickly and lead to a better recovery even after shear rate is removed. Thus, samples formulated with synthesized silver nanoparticles are said to have a strong thixotropic behaviour and have high stability. In addition, it was observed that both S3 and S7 that were formulated with commercial silver nanoparticles of 20 nm have higher percentage of recovery after shear is removed than both S2 and S6 that were formulated with commercial silver nanoparticles of 10 nm. This clearly shows that as filler sizes increase, the recovery percentage after shear is removed will increase too.

$$\text{Recovery}\,(\%) = 100 - \left[\frac{\text{Viscosity}\,(\text{rest}) - \text{Viscosity}\,(\text{recovery})}{\text{Viscosity}\,(\text{rest})} \times 100\%\right] \quad (10)$$

Table 7.1: Percentage of recovery after removal of shear rate (%) for all formulated ICAs

Samples	Formulation	Percentage of recovery after removal of shear rate (%)
S1	0.4-DGEBA/0.6-silver flakes	89.90
S2	0.4-DGEBA/0.5-silver flakes + 0.1-silver nanoparticles 10nm	80.03
S3	0.4-DGEBA/0.5-silver flakes + 0.1-silver nanoparticles 20nm	87.67
S4	0.4-DGEBA/0.5-silver flakes + 0.1-synthesize silver nanoparticles	90.40
S5	0.2-DGEBA/0.6-silver flakes	93.99
S6	0.2-DGEBA/0.7-silver flakes + 0.1-silver nanoparticles 10nm	95.21
S7	0.2-DGEBA/0.7-silver flakes + 0.1-silver nanoparticles 20nm	93.46
S8	0.2-DGEBA/0.7-silver flakes + 0.1-synthesize silver nanoparticles	94.54

CHAPTER 8

SUMMARY, CONCLUSION AND FURTHER WORK

8.1 Introduction

This chapter presents the summary, conclusions and suggestions for future work of the study conducted on the rheological characterisations of isotropic conductive adhesives (ICAs) for Microelectronic Packaging Applications.

8.2 Summary

The summary section is separated into four main sections. It includes, the summary of findings from the synthesis of silver nanoparticles for ICAs, the investigation of the empirical modelling of silver nanoparticles based ICAs, the study of viscoelastic behaviour of pastes, and the study of thixotropic behaviour of pastes.

8.2.1 Synthesis of silver nanoparticles for ICA pastes

Synthesized silver nanoparticles in lab can not only reduce the production cost, but also to produce a colloidal silver nanoparticles solution with a range of different size. Silver salts have been done by varieties of chemical reduction methods (Arnim and Michael, 1999; Andreescu et al., 2007; Solomon et al., 2007). The reduction of silver nitrates by sodium borohydride was able produce a colloidal silver nanoparticles that presents in bright yellowish colour. In this study finding, the stock materials, which are aqueous silver nitrate and aqueous sodium borohydride must be prepared in low concentration. This is due to the high concentration for aqueous silver nitrate and aqueous sodium borohydride will cause the equilibrium of the equation shift to the right immediately and form large agglomeration of silver nanoparticles during the reduction process. The colloidal silver exhibited an intense and absorption peak at wavelength 380 nm as measure by UV-Vis spectroscopy. A further confirmation was done with EDX spectra to ensure the presence of silver nanoparticles in the colloidal system after reduction of sodium borohydride with silver nitrate. The FE-SEM images clearly show that synthesize silver nanoparticles range from 10 nm to 20 nm.

8.2.2 Study of the effects of filler size and weight fraction on viscosity and the empirical modelling of silver nanoparticles based ICA pastes

The relationship between the viscosity and fillers weight fraction is clarified. As the concentration of filler increase, the amount of particles within the system increase, hence, the inter-particles interactions increase too. Formulated ICAs with 0.8 weight fraction shows a higher viscosity if compare to ICAs with 0.6 weight fraction. The increase of silver nanoparticles size in the formulation of ICA leads to an increases in viscosity. In addition, due to synthesized silver nanoparticles having a size range of 10 nm to 20 nm, the formulated ICAs (S4 and S8) has the highest viscosity among all others sample within the group of same weight fraction. This is because the silver nanoparticles is well dispersed into the system. Among all the empirical models, Cross model fitted best with the experimental data with the highest correlation coefficient value, R^2. The effect of weight fraction and size of filler are important elements that can be used to improve the new ICAs formulation in future for manufacture purpose.

8.2.3 Study of viscoelastic behaviour of silver nanoparticles based ICA pastes

To understand the rheological properties of ICAs, the effect of filler weight fraction and filler size on the viscoelastic behaviour of isotropic conductive

adhesives (ICAs) were investigated in this study. The results show all formulated ICAs has a storage modulus, G' that is higher than loss modulus, G". This indicates all samples have a more solid-like behaviour before shear was applied. As the shear applied increases, the formulated ICAs gradually change from solid-like behaviour to liquid-like behaviour. This is due to the inter-particles interaction that starts to breakdown within the flux system. The solid characteristics (G') and liquid characteristics (G") of the pastes measured in the oscillatory sweep test may explain how well a ICAs paste performs during the withdrawal of a printing process. The measured data could determine the formation of sediment in the ICA.

The ratio G"/G' provides an indication of interaction strength within the internal structure of a flux system. A material that is elastic in nature will has a lower G"/G' ratio. ICAs formulated with synthesized silver nanoparticles have the lowest G"/G' ratio. This indicates that synthesize silver nanoparticles that have a size range of 10-20 nm disperse well enough in the flux system, hence, they are more elastic than others formulation. Another parameter examined is the stress at G'= G" which also named as yield point. It is an important cohesive indicator of an ICAs. The results show that ICAs with a higher degree of cohesiveness has a higher value of yield point. This indicates that the formulated ICAs require a significant amount of stress in order for it to change from a solid state to a liquid state. The results from this study showed that the ICAs formulated with synthesized silver nanoparticles have the highest yield points. This indicates that such ICAs has the strongest particle interaction than

others samples. Thus, more stress is necessary to squeeze the paste to release from the aperture during the printing process.

The phase angle of the paste provides a better understanding of the transition from solid-like to liquid-like behaviour of a suspension. In brief, a paste with a lower phase angle may be very tacky and a paste that has a high phase angle may easily slump during the printing process. Among all the formulated ICAs, S4 and S8 formulated with synthesized silver nanoparticles have the lowest phase angle, which is 34.6 and 30.2. This indicates that these pastes are being high cohesive or tacky. This is due the synthesize silver nanoparticles has a size range of 10 nm to 20 nm that allow each particle to fill in the gap in between. Hence, reduction of flocs and lead to a stronger attraction among each particle in the system. Monitoring properties such as viscoelastic behaviour is significantly important for engineers to increase the yield because it provides a reliable and consistent printing performance during microelectronic packaging at all times.

8.2.4 Study of thixotropic behaviour of silver nanoparticles based ICA pastes

In this study, the viscosity of formulated ICAs was examined to identify the effect of shear rate on the thixotropic behaviour of the paste. This allows us to correlate the ICAs rheological properties to the printing performance. The

thixotropic test method is useful to evaluate the pastes thixotropic behaviour with respect to its printability during microelectronic packaging. A few different parameters were studied in the formulation of ICAs such as the effect of filler concentration and filler size.

The hysteresis loop is formed by a down curve and up curve. The presence of this area within the loop indicates that the ICAs are thixotropic in nature. The results clearly show that all ICAs undergo shear thinning when shear is applied. In addition, ICAs S4 and S8 showed the largest area between the down and up curve. This indicates that both ICAs undergoes the largest structural breakdown, but yet shows that they have the best thixotropic behaviour as they have the best recovery among others samples. Hence, ICAs formulated with synthesized silver nanoparticles has a higher elastic behaviour as they show a very good recovery even after a large structural breakdown when the shear is removed. The finding from this study shows that the larger filler size result to an increase of packing stress and lead to a better inter-particle attraction. As the weight fraction of filler increase, the viscosities of the paste increase too. This study highlighted the importance of thixotropic in a printing process. The viscosity of a ICAs must be low enough to squeeze out from the squeegee but must be also high enough to reshape. The recovery of the pastes and structural breakdown are important parameters that allow engineers to improve the development of a new formulation of isotropic conductive adhesives.

8.3 Conclusions

A number of conclusions can be made from the results of the study presented in this thesis:

1) ICAs formulated with synthesized silver nanoparticles (size range between 10 nm to 20 nm) showed a high degree of thixotropic (structural breakdown).
2) ICAs formulated with synthesized silver nanoparticles (size range between 10 nm to 20 nm) showed high elasticity behaviour (great recovery).
3) ICAs with 0.8 weight fraction showed more solid-like behaviour and stable dispersion.
4) The results suggest that the formulated ICAs of 0.8 weight fraction of synthesize silver nanoparticles are more promising for the stencil printing process (can be breakdown easily and great recovery with high viscosity).

8.4 Suggestion for Future Work

The rheological characterisation of isotropic conductive adhesives (ICAs) used for Microelectronic Packaging Applications has been reported in this thesis. The characterisation of the ICAs and its correlation to the formulation

materials is a very complex assignment. Here are some suggestions for possible further work within this area:

1) The commercial silver nanoparticle is very useful in research. However, commercial silver nanoparticles come with a specific size and this may result in a very high production cost for a study. Synthesized silver nanoparticles in the laboratory enable us to obtain the specific range of silver nanoparticles with a lower production cost. It requires a large amount of ice cold sodium borohydride to reduce the ionic silver and also to stabilize the formed silver nanoparticles. Reducing the concentration of aqueous silver nitrate and aqueous sodium borohydride ensures that the colloidal silver nanoparticles can be obtained. A high concentration of the two materials will shift the equilibrium to right immediately and form silver nanoparticles that is in solid state instead of in colloidal aqueous. In this study, the effects of size of material concentration and temperature of silver nitrate and sodium borohydride on synthesizing silver nanoparticles were examined and the results suggested that material concentration and temperature strongly affected the size range of the synthesize silver nanoparticles. Further work is suggested to synthesize silver nanoparticles with other methods to produce silver nanoparticles that are in specific shape such as nanoprisms or nanosphere to allow us to identify their effect on rheology properties of ICAs.

2) Rheology is an approach to describe how well an adhesive perform in ‘real world’ application. In most cases, the rheology can be described by the viscosity of a suspension when shear is applied. In some other cases, the thixotropy of a suspension is used to described it too. Thixotropic materials are characterised by the fact that when the suspension are stable when there are no shear or stress is applied, but they become more or less viscous when stress start to apply to them such as stirring or unloading. By adjusting the concentration of filler, the filler particles’ properties, and mixing different types of additives, most likely it should be able to achieve a suitable rheology for microelectronic printing. In this study, the effects of filler size and its weight fraction on rheology of ICAs were examined and the results show that filler size and concentration affect the viscosity of ICAs significantly.

List of References

Andreescu, D., Eastman C., Balantrapu K. and Goia, D. V., 2007. A simple route for manufacturing highly dispersed silver nanoparticles. *Journal of materials research*, 22(9), pp. 2488 – 2496.

Andrew, S, 2001. *An Introduction to Fluid Mechanics*. Leeds: University of Leeds.

Agote, I., Odriozola A., Gutierrez, M., Santamaria, A., Quintanilla, J. and Coupella, P., 2001. Rheological study of waste porcelin feedstocks for injection moulding. *Journal of the European Ceramics Society*, 21 (16), pp. 2843 - 2853.

Arash, M., 2013. The effect of functionalization on the viscoelastic behavior of multi-wallcarbon nanotube/epoxy composites. *Materials and Design*, 45, pp. 510-517.

Arild, S. et al., 2012. Viscoelastic Properties of Oil-Based Drilling Fluids. *Annual Transactions of the Nordic Rheology Society*, 20, pp. 33-47.

Arnim, H. and Michael, G., 1999. Formation of colloidal silver nanoparticles: Capping action of citrate. *The Journal of Physical Chemistry B*, 103 (44), pp. 9533 – 9539.

Asta, A., Judita, P., Igoris, P. and Sigitas, T., 2009. Investigation of silver nanoparticles formation kinetics during reduction of silver nitrate with sodium citrate. *Materials Science*, 15(1), pp. 21 - 27.

Bahadory, M., 2008. *Synthesis of noble metal nanoparticles*. PhD thesis, Drexel Univeristy, USA.

Barnes, H. A., 1997. Thixotropic a review. *Journal Non-Newtonian Fluid Mechanic*, 70 (1), pp. 1 - 33.

Batchelor, G. K., 1970. *An introduction to fluid dynamics*. UK: Cambridge University Press.

Bearbeitet, V.J.P.P. and Williams, J.J., 2010. *Epoxy Polymers*. Germany: Wiley.

Behzadfar, E., Abdolrasouli, M.H., Sharif, F. and Nazockdast, H., 2009. Effect of solid loading and aggregate size on the rheological behavior of PDMS/Calcium carbonate suspensions, *Brazilian Journal of Chemical Enginering*, 26 (4), pp. 713 – 721.

Bryan, B., Witold, B. and Kevin, P.M., 1999. Epoxy Thermosets and Their Applications I: Chemical Structures and Applications. *Journal of Materials Education*, 21 (5-6), pp. 281-286.

Bönnemann. H. and Ryan, M. R., 2001. Nanoscopic metal particles - synthetic methods and potential applications. *European Journal of Inorganic Chemistry*, (10), pp. 2455 – 2480.

Bullard, J. W., Pauli, A.T., Garboczi, E.J. and Martys, N. S., 2009. Comparison of viscosity-concentration relationships for emulsions. *Journal of Colloid and Interface Science*, 330, pp. 186 - 193.

Cheng, W.T., Chih, Y.W. and Yeh W.T., 2007. In Situ Fabrication of Photocurable Conductive Adhensives with Silver Nanoparticles in The Absence of Capping Agent. *International Journal of Adhesion & Adhesives*, 27, pp. 236-243.

Dahlback, L.M. and Lundstrom, S., 1995. A method to measure wetting between resin and reinforcement. *Proceedings of the Tenth International Conference on Composite Materials: [Proceedings of ICCM-10]*, 14 - 18 August 1995 Whistler, British Columbia. Canada: Vancouver, pp. 293 - 300.

Durairaj, R., Ekere, N.N. and Salam, B., 2004. Thixotropy flow behaviour of solder and conductive adhesives paste. *Journal of Material Science: Materials in Electronic*, 15, pp. 677.

Durairaj, R., Jackson G.J., Ekere, N.N., Glinski, G. and Bailey, C., 2002. Correlation of solder paste rheology with computational simulations of the stencil printing process. *Soldering and Surface Mount Technology*, 14 (1), pp. 11 - 17.

Durairaj, R., Mallik, S., Seman, A., Marks, A. and Ekere, N.N., 2009. Rheological characterisation of solder pastes, isotropic conductive adhesives used for flip chip assembly. *Journal of Materials and Processing Technology*, 209, pp. 3923 - 3930

Durairaj, R., Mallik, S., Seman, A., Marks, A. and Ekere, N.N., 2009. Rheological characterisation of Sn/Ag/Cu solder pastes. *Journal of Materials and Design*, 30, pp. 3812 - 3818.

Elaine, et al., 2006. A simple model to describe the thixotropic behavior of paints. *Progress in Organic Coatings*, 57 (3), pp. 229-235.

Evans, J. and Beddow J., 1987. Characterisation of particle morphology and rheological behaviour in solder paste. *IEEE Transactions on Components, Hybrid, and Manufacturing Technology*, 10 (2), pp. 224 - 231.

Fang, Y., 1998. Optical absorption of nanoscale colloidal silver: aggregate band and adsorbate-silver surface band. *Journal of Physical Chemistry,* 1998, 108, pp. 4315 - 4318.

Ferguson, J. and Kemblowski, Z., 1991. *Applied Fluid Rheology*. New York: Elsvier Applied Science.

Gilleo, K., 1995. Assembly with Conductive Adhesives. *Soldering and Surface Mount Technology*, 19, pp. 12 - 17.

Goertzen, W.K. and Kessler, M.R., 2006. Creep behaviour of Carbon Fiber/Epoxy Matric Composite. *Materials Science and Engineering*: A, 421 (1-2), pp. 217-225.

Gosta, B, 1995. *Dairy Processing Handbook*. Sweden: Tetra Pak Processing Systems.

Green, H. and Weltmann, R.N., 1946. Industrial Rheology and Reologieal Structures. *Ind. Eng. Chem. Anal. Ed.* 18, pp. 167 - 172.

Haitham, E., Satterthwaite, J. and Silikas, N., 2011. Effect of filler size and temperature on packing stress and viscosity of resin-composites. *Int. J. Mol. Sci*, 12, pp. 5330 – 5338.

Holter, O., Finn, I. and Hugo. P., 1998. Fysikk og energiressurser. *Universitetsforlaget*, 2nd edition.

Hongshui, W., Qiao, X., Chen, J., Wang, X. and Ding, S., 2005. Mechanisms of PVP in the preparation of silver Nanoparticles. *Materials Chemistry and Physics*, pp. 449 - 453.

Huang, H.H. et al., 1996. Photochemical formation of silver nanoparticles in PVP. *Langmuir*, 12, pp. 909 - 912.

Hvims, H.L., 1995. Conductive Adhesives for SMT and Potential Applications. *IEEE Transactions on Components, Packaging, and Manufacturing Technology Part B*, 18 (2), pp. 284 - 291.

Ineke, V.T.A., and Eli, W., 2003. *Thixotropy of Solder Paste Impacts Repeatability and Reproducibility of Rheometric Results*. Germany: Balver Zinn.

Irfan, M. and Kumar, D., 2008. Recent advances in isotropic conductive adhesives for electronics packaging applications. *International Journal of Adhesion & Adhesives*, 28, pp. 362 - 371.

Jan, E., Colin S. and Adam S.B., 2005. Squeeze flow theory and applications to Rheometry. *Journal of Non-Newtonian Fluid Mechanics*, 132, pp. 1 - 27.

Jagt, J.C., 1999. *Conductive Adhesives for Electronics Packaging*. Bristol: Electrochemical Publications Ltd.

Jon, E.W. 2009. Rheological Properties of Cement Paste: Thixotropic Behaviour and Structural Breakdown. *Cement and Concrete Research*, 39, pp. 14-29.

Kamat, P.V., Flumiani, M. and Hartland, G.V., 1998. Picosecond dynamics of silver nanoclusters and Photoejection of electrons and fragmentation. *Journal of Physical Chemistry. B*, 102, pp. 3123 – 3128.
Kim, J.H., Satoh, M. and Iwasaki, T., 2005. Rheological properties of particle-flux suspension paste. *Advanced Powder Technology*, 16, pp. 61 - 71.

Kim, W.J., Taya, M., and Nguyen, M.N., 2009. Electrical and thermal conductivities of a silver flake/thermosetting polymer matrix composite. *Mechanics of Materials*, 41 (10), pp. 1116–1124.

Kirkwood D.H. and Ward P.J., 2007. Comment on the power law in rheological equations. *Material Letters*, 62, pp. 3981 - 3983.

Klosterman, D., and Li, L., 1996. Conduction and Microstructure Development in Ag Filled Epoxies. *Journal of Electronics Manufacturing*, 5 (4), pp. 277 - 287.

Koszkul J. and Nabialek J., 2004. Viscosity models in simulation of the filling stage of the injection molding process. *J. Materials Processing Technology*, 157 (158), pp. 183-187.

Kottaus, S., Guenther B.H., Haug, R. and Schafer, H., 1997. Study of Isotropically Conductive Bondings Filled with Aggregates of Nano-Sized Ag-Particles. *IEEE Transactions on Components, Packaging, and Manufacturing Technology*, Part A, 20 (1), pp. 15-20.

Kusy, R.P. and Leinfelder, K.F., 1977. Pattern of wear in posterior composite restorations. *Journal of Dental Research*, 56, pp. 544.

Lapasin, R., Sabrina, P., Vittorio, S. and Donato, C., 1997. Viscoelastic properties of solder pastes. *Journal of Electronic Materials*, 27, pp. 138-148.

Larson, R.G., 1999**.** The structure and rheology of complex fluids. *Topics in Chemical Engineering*. New York: Oxford Press. Inc., pp. 263 - 272.

Li, L., Lizzul, C., Kim, H., Sacolick, I. and Morris, J.E., 1993. Electric, structure and processing properties of electrically conductive adhesives. *IEEE Transactions on Components, Hybrids, and Manufacturing Technology*, 16 (8), pp. 843.

Li, T.P., Tan, Y.R.J., Breach, C.D. and Hawkins, A., 2014. The Rhelogy and Printing Behaviour of Water Soluble Solder Pastes. *Journal of Surface Mount Technology*

Liu, J., 1999. Conductive Adhesives for Electronics Packaging. *Port Erin, Isle of Man*, British Isles: Electrochemical Publications LTD.

Liu, J., Gustafsson, K., Lai, Z. and Li, C., 1997. Surface Characteristics, Reliability, and Failure Mechanisms of Tin/Lead, Copper, and Gold Metallizations. *IEEE Transactions on Components, Packaging, and Manufacturing Technology, Part A*, 20, pp. 21 - 30.

Liu, J. and Lai, Z., 1998. Overview of Conductive Adhesive Joining Technology in Electronics Packaging Applications. *3rd International Conference on Adhesive Joining and Coating Technology in Electronics Manufacturing*, pp. 1 – 17.

Lu, D.D. and Wong, C.P., 2000. Development of Conductive Adhesives Filler with Low-melting-point Alloy Fillers *International Symposium on Advanced Packaging Materials*, 6 – 8 March 2000 Port Erin, Isle of Man. British Isles, pp. 7 – 13.

Lu D.D. and Wong C.P., 2008. Recent Advances in Developing High performance isotropic Conductive Adhesive. *J. Adhesion Sci. Technol*, 22, pp. 835– 851.

Lyons, A.M., 1991. Electrically Conductive Adhesives: Effect of Particle Composition and Size Distribution. *Polymer Engineering and Science*, 31 (6), pp. 445 - 450.

Malucelli, G et al., 2007. Intercalation effects in LDPE/o-montmorillonites nanocomposites. *European Polymer Journal*, 43, pp. 328 - 335.

Malynych, S., Luzinov, I. and Chumanov, G., 2001. Poly(vinyl pyridine) as universal surface modifier for immobilization of nanoparticles. *Journal of Physical Chemistry B*, 106 (6), pp. 1280-1285.

McGrath, L.M., et al., 2008. Investigation of the thermal, mechanical and fractureproperties, of alumina-epoxy composites. *Polymer*. 49, pp. 999 - 1014.

McLelland, A.R.A., Henderson, N.G., Atkinson, H.V. and Kirkwood, D.H., 1997. Anomalous rheological behavior of semi-solid alloy slurries at low shear rates. *Materials Science and Engineering*, A232, pp. 110 - 118.

Meier, J., et al., 2002. Microcrystalline silicon and the impact on micromorph tan- dem solar cells. *Solar Energy Materials and Solar Cells*, 74 (11), pp. 457 – 467.

Mewis, J. and Wagner, N.J., 2009. Current trend in suspension rheology. *Journal of Non-Newtonian Fluid Mechanical*, 157, pp. 147.

Mongomery, D.C., Peck, E.A. and Vining, G.G., 2001. *Introduction to Linear Regression Analysis.* 3rd ed. New York: John Wiley & Sons Inc.

Nair, A.S. and Pradeep, T.Y, 2003. Halocarbon mineralization and catalytic destruction by metal nanoparticles. *Current Science*, 84, pp. 1560.

Nauchbaur, L., Mutin, J. G., Nonat, A. and Choplin, L., 2001. Dynamic mode rheology of cement and tricalcium silicate pastes from mixing to setting. *Journal of Polymer Composites,* 31, pp. 183 - 192.

Nguty, T.A., Ekere, N.N. and Adebayo, A., 1999. Correlating solder paste composition with stencil printing performance. *In: IEEE/CPMT International Electronics Manufacturing Technology Symposium*, 18 – 19 October 1999 Austin, Texas, pp. 301 – 309.

Nguyen, Q.H. and Nguyen N.D., 2012. *Incompressible Non-Newtonian Fluid Flows*. Continuum Mechanics - Progress in Fundamentals and Engineering Applications. Toledo: InTech.

Orthmann, K., 1999. Electrical and Mechanical Properties of Conductive Adhesive Bonds in Comparison with Soldering in PCB Technology, H. Vogel, München, Germany, 1991 (in German).
Perichaud, M.G., Deletage, J.Y., Fremont, H., Danto, Y. and Faure, C., 2000. Reliability Evaluation of Adhesive Bonded SMT Components in Industrial Applications. *Microelectronics Reliability*, 40, pp. 1227 - 1234,

Phuapradit, W., Shah, N.H., Lou, Y., Kundu, S., and Infeld, M.H., 2002. Critical processing factors affecting rheological behaviour of a wax based formulation. *European Journal of Pharmaceuticals and Biopharmaceuticals*, 53 (2), pp. 175-179.

Rajinder, P., 2005. Modelling viscoelastic behavior of particulate composites with high volume fraction of filler. *Materials Science and Engineering:A*, pp. 71 - 77.

Rao, M.A., 2007. *Rheoloy of Fluid and Semisolid Foods: Principle and Applications*, Springer, 2, pp. 27 - 120.

Rao M.A., 2014. *Rheology of Fluid, Semisolid, and Solid Foods,* Food Engineering Series. New York: Springer Science+Business Media.

Rebeca, G., 2010. On The Influence of Silver Nanoparticles Size in the Electrical Conductivity of PEDOT:PSS. *Material Science Forum*, 644, pp. 85-90.

Ritter, G.W., 1999. Electrical Current Effects on Conductive Eposies. *Proceedings of the 22nd Annual Meeting of the Adhesion Society*, pp. 56 – 59.

Rusanen, O., 2000. Modelling of ICA creep properties. *Proceeding of 4th International Conference on Adhesive Joining & Coating Technology in Electronics Manufacturing*, 18 – 21 June 2000. Espoo, Finland, pp. 194-198.

Shahzada, A., Bohidar, H.B. and Agnihotry, S.A., 2006. Role of Fumed Silica on ion conduction and rheology in nanocomposite polymeric electrolytes. *Polymer*. Pp. 3583 - 3590.

Shimada, Y., Lu, D. and Wong, C. P., 2000. Electrical Characterizations and Considerations of Electrically Condutive Adhesives (ECAs). *International Symposium on Advanced Packaging Materials*, pp. 336-342.

Shirtcliffe, N., Nickel, U. and Schneider, S., 1999. Reproducible preparation of silver sols with small particle size using borohydride reduction: for use as nuclei for preparation of larger particles. *Journal of Colloid and Interface Science*, 211, pp. 122 - 129.

Solomon, S. et al., 2007. Synthesis and study of silver Nanoparticles. *Journal of Chemical Education*, 84 (2), pp. 322-325.

Tsung N.T., 2007. A Knowledge-Based System for Stencil Printing Process Planning and Control. *Journal of the Chinese Institute of Inductrial Engineers*, 12(6), pp. 513 - 521.

Van Hyning, D. L., and Zukoski, C. F., 1998. Formation mechanisms and aggregation behavior of borohydride reduced silver particles. *Langmuir*, 14, pp. 7034 - 7046.

Van Hyning, D.R., Klemperer, W.G., and Zukowski, C.F., 2001. Characterization of colloidal stability during precipitation reactions, *Langmuir*, 17, pp. 3120 – 3127.

Wang, D.B., Song, C., Hu, Z., and Zhou, X., 2005. Synthesis of silver nanoparticles with flake-like shapes, *Materials Letters*, 59 (14-15), pp. 1760 - 1763.

Wilhelm, M., 2002. Fourier-transform rheology. *Macromol Mater Eng*. 287, pp. 83-105.

Wong, C.P. and Yi Li., 2006. Recent advances of conductive adhesives as a lead-free alternative in electronic packaging: Materials, processing, reliability and applications. *Material Science and Engineering*, 51, pp. 1 - 35.

Xiong, Y.J. et al., 2006. Poly(vinyl pyrrolidone): A dual functional reductant and stabilizer for the facile synthesis of noble metal nanoplates in aqueous solutions. *Langmuir*, 22 (20), pp. 8563 - 8570.

Yim, B. S. and Kim, J.M., 2010. Characteristics of Isotropically Conductive Adhesive (ICA) Filled with Carbon Nanotubes (CNTs) and Low-Melting-Point Alloy Fillers. *Materials Transactions*, 51 (12), pp. 2329-2331.

Yu, A.K., Kudrinskiy, A.A., Olenin, A.Y. and Lisichkin G.V., 2008. Synthesis and properties of silver nanoparticles: advances and prospects. *Russian Chemical Reviews*, 77 (3), pp. 233.
Zhang, S.S., Zhang, Y.J. and Wang, H.W., 2010. Effect of particle size distributions on the rheology of Sn-Ag-Cu lead-free solder pastes. *Material and Design*, 31, pp. 594-598.

Zheng, S., Pascault, J.P., Williams, R.J.J., 2010. *Epoxy Polymers. New Materials and Innovations*, London: Wiley-VCH.